Scalar-tensor theories of gravity, neutrino physics, and the H_0 tension

Mario Ballardini,[a,b,c,d,1] **Matteo Braglia,**[a,b,c] **Fabio Finelli,**[b,c]
Daniela Paoletti,[b,c] **Alexei A. Starobinsky**[e,f] **and Caterina Umiltà**[g]

[a]Dipartimento di Fisica e Astronomia, Alma Mater Studiorum Università di Bologna,
 via Gobetti 93/2, I-40129 Bologna, Italy

[b]INAF/OAS Bologna,
 via Piero Gobetti 101, I-40129 Bologna, Italy

[c]INFN — Sezione di Bologna,
 via Irnerio 46, I-40126 Bologna, Italy

[d]Department of Physics & Astronomy, University of the Western Cape,
 Cape Town 7535, South Africa

[e]Landau Institute for Theoretical Physics,
 119334 Moscow, Russia

[f]Bogolyubov Laboratory of Theoretical Physics, Joint Institute for Nuclear Research,
 141980 Dubna, Moscow Region, Russia

[g]Department of Physics, University of Illinois Urbana-Champaign,
 Urbana, IL 61801, U.S.A.

 E-mail: mario.ballardini@inaf.it, matteo.braglia2@unibo.it, fabio.finelli@inaf.it,
 daniela.paoletti@inaf.it, alstar@landau.ac.ru, umilta@illinois.edu

Abstract. We use *Planck* 2018 data to constrain the simplest models of scalar-tensor theories characterized by a coupling to the Ricci scalar of the type $F(\sigma)R$ with $F(\sigma) = N_{\rm pl}^2 + \xi\sigma^2$. We update our results with previous *Planck* and BAO data releases obtaining the tightest constraints to date on the coupling parameters, that is $\xi < 5.5 \times 10^{-4}$ for $N_{\rm pl} = 0$ (induced gravity or equivalently extended Jordan-Brans-Dicke) and $(N_{\rm pl}\sqrt{8\pi G}) - 1 < 1.8 \times 10^{-5}$ for $\xi = -1/6$ (conformal coupling), both at 95% CL. Because of a modified expansion history after radiation-matter equality compared to the ΛCDM model, all these dynamical models accommodate a higher value for H_0 and therefore alleviate the tension between *Planck*/BAO and distance-ladder measurement from SNe Ia data from 4.4σ at best to 2.7-3.2σ with CMB alone and 3.5-3.6σ including BAO data. We show that all these results are robust to changes in the neutrino physics. In comparison to the ΛCDM model, partial degeneracies between

---

[1]Corresponding author.

neutrino physics and the coupling to the Ricci scalar allow for smaller values $N_{\rm eff} \sim 2.8$, 1σ lower compared to the standard $N_{\rm eff} = 3.046$, and relax the upper limit on the neutrino mass up to 40%.

Contents

1 Introduction

The distance-ladder measurement of the Hubble constant from supernovae type Ia (SNe Ia) [1, 2] and from strong-lensing time delays [3–5] disagrees with the value inferred from the fit of the cosmic microwaves background (CMB) anisotropies [6, 7]. In particular, the value inferred using the *Planck* legacy data for a flat ΛCDM cosmological model, $H_0 = (67.36 \pm 0.54)$ km s^{-1}Mpc^{-1} [7], is in a 4.4σ tension with the most recent measurement from the SH0ES team [8], that is $H_0 = (74.03 \pm 1.42)$ km s^{-1}Mpc^{-1}, determined using Cepheid-calibrated SNe Ia with new parallax measurements from HST spatial scanning [2] and from Gaia DR2 [9], in a 3.2σ tension with the strong-lensing time delay determination from the H0LiCOW collaboration [5], that is $H_0 = \left(73.3^{+1.7}_{-1.8}\right)$ km s^{-1}Mpc^{-1}, and in a 5.3σ tension with the combined SH0ES + H0LiCOW value $H_0 = (73.8 \pm 1.1)$ km s^{-1}Mpc^{-1} [5].

Although it does not seem possible to completely solve the discrepancy between CMB and local measurements by considering unaccounted systematic effects [10–12], revisions of the determination of the Hubble rate based on the Cepheid calibration [13–15], and from SNe Ia calibrated using the tip of the red giant branch method [16] point to values which are still higher than the *Planck* measurements, i.e. ~ 70 km s^{-1}Mpc^{-1}, but to a smaller extent (see however [17–21] for more recent developments).

Alternatively, the H_0 *tension* can be addressed by evoking new physics beyond the ΛCDM concordance model, either in the late or early time Universe [22, 23]. Late-time modifications include a phantom-like dark energy (DE) component [24–26], a vacuum phase

transition [27–31], interacting dark energy [32–36], or quintessence in a non-flat Universe [37]. However, these models are tightly constrained [1, 25, 33, 38] by late-time observational data, especially those from baryon acoustic oscillations (BAO) [39–41].

With the highly precisely determined angular scale of the last-scattering surface (LSS) [42], it has been suggested that a smaller value of the comoving sound horizon at baryon drag r_s can provide a higher value of H_0 without spoiling the CMB angular power spectrum measurements and without changing the BAO observables [23, 43]. An example of such an early-time modification is the extension to additional light relics, eventually interacting with hidden dark sectors [44–51]. Another promising early-time solution, is an exotic early dark energy (EDE) component that remains subdominant for the majority of the cosmological evolution of the Universe and injects a small amount of energy in a very narrow redshift window [52–57]. Note that features in the primordial power spectrum [58, 59] and modifications of the recombination history [60, 61] are not able to increase H_0.

Another interesting possibility is to alleviate the H_0 *tension* through a modification of General Relativity (GR) [62–71], which can include early- and late-time modifications of the expansion history with respect to ΛCDM. Scalar-tensor theories of gravity that involve a scalar field non-minimally coupled to the Ricci scalar naturally change the effective relativistic degrees of freedom in the radiation-dominated epoch and the background expansion history from ΛCDM, thus leading to a higher CMB-inferred H_0 [62, 63, 66]. This has been shown for the extended Jordan-Brans-Dicke (eJBD) model in refs. [62, 63] where the cosmological parameters estimation has been carried out using data from the *Planck* 2013 and 2015 release respectively. The robustness of a higher H_0 in these theories has been proved in ref. [66], where a more general form of the non-minimal coupling (NMC) to gravity has been considered. In this paper, we confirm earlier results for the particular cases of eJBD and a conformally coupled (CC) scalar field using the most recent cosmological data.

Since the mechanism that drives a higher inferred H_0 relies on the radiation-like behavior of the scalar field at early times, it is interesting to investigate to what extent these simple scalar-tensor theories are degenerate with effective number of relativistic species due to neutrinos and to any additional massless particles produced well before recombination $N_{\rm eff}$. The current tight constraints from the latest *Planck* 2018 data $N_{\rm eff} = 2.89 \pm 0.19$ ($N_{\rm eff} = 2.99 \pm 0.17$ including BAO) at 68% CL [7] can be changed in modified gravity theories as previously shown in the context of $f(R)$ gravity in [72, 73].

While changing $N_{\rm eff}$ can lead to a higher value for H_0 compared with the value inferred in the ΛCDM model from the CMB anisotropies measurements, in the extension of ΛCDM model with non-zero total neutrino mass m_ν, lower values of H_0 correspond to higher values of m_ν and higher values of H_0 correspond to lower m_ν. For instance, the constraint from *Planck* 2018 data in combination with BAO data is $m_\nu < 0.12\,{\rm eV}$ at 95% CL [7, 74] and combining with the measurement from the SH0ES team the limit further tightens to $m_\nu < 0.076\,{\rm eV}$ [75]. In scalar-tensor theories of gravity, it is possible to keep fixed the angular diameter distance at decoupling or even increase it in order to recover a higher H_0 while increasing the total neutrino mass value [76]. Given that neutrino oscillations are the only laboratory evidence of physics beyond the Standard Model of Particle Physics [77], it is natural to ask ourselves either how the cosmological constraints on neutrino physics can be relaxed in these simple models of scalar-tensor theories compared to the ΛCDM concordance model and how much constraints become larger in the NMC models including the neutrino parameters.

Future CMB experiments, such as the Simons Observatory[1] [78], CMB-S4[2] [79], and future LSS surveys from DESI[3] [80], Euclid[4] [81, 82], LSST[5] [83], SKA[6] [84, 85] will help to improve the constraints on these extended cosmologies [86–88] and limit the degeneracy of neutrino parameters $N_{\rm eff}$ and m_ν with scalar-tensor theories [89].

The paper is organized as follows. Section 2 is devoted to a description of the models considered. We describe the datasets considered in section 3. In in section 4, we start by discussing the updated constraints on the eJBD and CC model in light of new CMB and BAO data, then we discuss the combination with the distance-ladder measure of H_0 from SNe Ia in section 5. We further improve the analysis by extending the cosmological parameters to the ones describing the neutrino sector in sections 6.1–6.2–6.3. We draw our conclusions in section 7. In appendix A, we collect all the tables with the constraints on the cosmological parameters obtained with our MCMC analysis.

2   The model: non-minimally coupled scalar-tensor theory

As far as cosmological tests are concerned, one of workhorse models to test deviations from GR is the eJBD [90, 91] theory, which has been extensively studied [62, 63, 67, 92–97]. NMC eJBD theory is perhaps the simplest extension to GR within the more general Horndeski theory [98]:

$$S = \int {\rm d}^4x \sqrt{-g} \left[\frac{F(\sigma)}{2} R - \frac{g^{\mu\nu}}{2} \partial_\mu \sigma \partial_\nu \sigma - V(\sigma) + \mathcal{L}_m \right] , \tag{2.1}$$

where $F(\sigma) = N_{\rm pl}^2 + \xi \sigma^2$, R is the Ricci scalar, and $\mathcal{L}_m$ is the Lagrangian density for matter fields. As in [66], we do not consider a quintessence-like inverse power-law potential (see for instance [99–103]), but we restrict ourselves to a potential of the type $V(\sigma) = \lambda F^2(\sigma)/4$ for which the scalar field is effectively massless. Our choice reduces to eJBD theory after the redefinition $\sigma^2 = \phi/(8\pi\xi)$, $\xi = 1/(4\omega_{\rm BD})$, and setting $N_{\rm pl} = 0$.

For a flat Friedmann-Lemaître-Robertson-Walker (FLRW) Universe with ${\rm d}s^2 = -{\rm d}t^2 + a^2(t){\rm d}\mathbf{x}^2$, the background Friedmann equations in the Jordan frame are [104]:

$$3FH^2 = \rho_m + \frac{\dot\sigma^2}{2} + V(\sigma) - 3H\dot{F} , \tag{2.2}$$

$$-2F\dot{H} = \rho_m + \dot\sigma^2 + \ddot{F} - H\dot{F} . \tag{2.3}$$

These equations are supplemented by the Klein-Gordon equation that governs the evolution of the scalar field:

$$\Box \sigma - V_\sigma + F_\sigma R = 0 . \tag{2.4}$$

The coupling between gravity and the scalar degree of freedom induces a time varying Newton's gravitational constant G_N, which is given by $G_N = 1/(8\pi F)$. This quantity is usually denoted by the cosmological Newton's gravitational constant, as opposed to the one that is actually measured in laboratory Cavendish-type experiments which is rather given by [104]:

$$G_{\rm eff} = \frac{1}{8\pi F} \frac{2F + 4F_{,\sigma}^2}{2F + 3F_{,\sigma}^2} . \tag{2.5}$$

---

[1]https://simonsobservatory.org/

[2]https://cmb-s4.org/

[3]http://desi.lbl.gov/

[4]http://sci.esa.int/euclid/

[5]http://www.lsst.org/

[6]http://www.skatelescope.org/

Deviations from GR for a theory of gravitation are parameterized by the so called post-Newtonian (PN) expansion of the metric [105]. In such an expansion, the line element can be expressed as:

$$ds^2 = -(1 + 2\Phi - 2\beta_{\mathrm{PN}}\Phi^2)dt^2 + (1 - 2\gamma_{\mathrm{PN}}\Phi)d\mathbf{x}^2\,, \tag{2.6}$$

where we have retained only the two non-null contributions to the PN expansion in the case of NMC theories, that is [104]

$$\gamma_{\mathrm{PN}} = 1 - \frac{F_{,\sigma}^2}{F + 2F_{,\sigma}^2}\,, \qquad \beta_{\mathrm{PN}} = 1 + \frac{FF_{,\sigma}}{8F + 12F_{,\sigma}^2}\frac{d\gamma_{\mathrm{PN}}}{d\sigma}\,. \tag{2.7}$$

Solar-system experiments agree with GR preditions, for which both γ_{PN} and β_{PN} are identically equal to unity, at a very precise level. Measurements of the perihelion shift of Mercury constrain $\beta_{\mathrm{PN}} - 1 = (4.1 \pm 7.8) \times 10^{-5}$ at 68% CL [105] and Shapiro time delay constrains $\gamma_{\mathrm{PN}} - 1 = (2.1 \pm 2.3) \times 10^{-5}$ at 68% CL [106].

In this paper we restrict ourselves to two simple models, both of which only contain one extra parameter with respect to the ΛCDM model: induced gravity (IG) described by $N_{\mathrm{pl}} = 0$ and $\xi > 0$, and a conformally coupled scalar field (CC) for which $\xi = -1/6$ and the free parameter is $N_{\mathrm{pl}} > M_{\mathrm{pl}}$. For both models, the effective value of the Newton's gravitational constant G_N decreases with time, whereas the scalar field σ increases for $\xi > 0$, e.g. for IG, and it decreases for $\xi < 0$, e.g. for CC.[7] We have $\gamma_{\mathrm{PN}} < 1$ and $\beta_{\mathrm{PN}} \leq 1$ for $\xi > 0$ ($\beta_{\mathrm{PN}} = 1$ for IG), whereas $\gamma_{\mathrm{PN}} < 1$ and $\beta_{\mathrm{PN}} > 1$ for $\xi < 0$.

In order to connect the present value of the field $\sigma_0 \equiv \sigma(z = 0)$ to the gravitational constant, we impose the condition $G_{\mathrm{eff}}(\sigma_0) = G$, where $G = 6.67 \times 10^{-8}$ cm^3 g^{-1} s^{-2} is the gravitational constant measured in a Cavendish-type experiment. This corresponds to

$$\tilde{\sigma}_0^2 = \frac{1 + 8\xi}{\xi(1 + 6\xi)} \tag{2.8}$$

for IG and

$$\tilde{\sigma}_0^2 = \frac{18\tilde{N}_{\mathrm{pl}}^2(\tilde{N}_{\mathrm{pl}}^2 - 1)}{1 + 3\tilde{N}_{\mathrm{pl}}^2}\,, \tag{2.9}$$

for the CC case. For simplicity, we denote quantities normalized to $M_{\mathrm{pl}} \equiv 1/\sqrt{8\pi G}$ with a tilde.

3 Methodology and datasets

In order to derive the constraints on the cosmological parameters we use a Markov Chain Monte Carlo (MCMC) analysis by using the publicly available code MontePython[8] [108, 109] connected to our modified version of the code CLASS[9] [110, 111], i.e. CLASSig [62]. Mean values and uncertainties on the parameters reported, as well as the contours plotted, have been obtained using GetDist[10] [112]. We use adiabatic initial conditions for the scalar field perturbations [66, 113].

---

[7]We refer the interested reader to refs. [62, 63, 66] for a detailed analysis of the background dynamics in these models, see also ref. [107] for the generalization to anisotropic homogeneous cosmological models of the Bianchi I type.

[8]https://github.com/brinckmann/montepython_public

[9]https://github.com/lesgourg/class_public

[10]https://getdist.readthedocs.io/en/latest

As baseline, we vary the six cosmological parameters for a flat ΛCDM concordance model, i.e. ω_b, ω_c, H_0, τ, $\ln\left(10^{10}A_s\right)$, n_s, plus one extra parameter related to the coupling to the Ricci curvature. For IG ($N_{\rm pl} = 0$, $\xi > 0$), we sample on the quantity $\zeta_{\rm IG} \equiv \ln\left(1 + 4\xi\right)$, according to [62, 63, 96] in the prior range [0, 0.039]. For CC ($N_{\rm pl} > M_{\rm pl}$, $\xi = -1/6$), we sample on $\Delta\tilde{N}_{\rm pl} \equiv \tilde{N}_{\rm pl} - 1$, according to [66], with prior range [0, 0.5]. In our updated analysis in section 4 we assume 3 massless neutrino with $N_{\rm eff} = 3.046$, but a more general neutrino sector is considered in the rest of the paper.

We quote constraints on the variation of the Newton's gravitational constant between the radiation era and the present time $\delta G_N/G_N$, and its derivative at present time $\dot{G}_N/G_N$. Defining the effective cosmological gravitational strength [95]:

$$\frac{G_N}{G}(z = 0) = \frac{1}{F(\sigma_0)}\,, \tag{3.1}$$

we have

$$\frac{\delta G_N}{G_N}(z = 0) = \frac{G_N(\sigma_0) - G_N(\sigma_{\rm ini})}{G_N(\sigma_{\rm ini})} = \frac{\sigma_{\rm ini}^2 - \sigma_0^2}{\sigma_0^2} \leq 0\,, \tag{3.2}$$

$$\frac{\dot{G}_N}{G_N}(z = 0) = -\frac{2\dot{\sigma}_0}{\sigma_0} \leq 0\,, \tag{3.3}$$

$$\frac{G_N}{G}(z = 0) = \frac{1 + 6\xi}{1 + 8\xi} \leq 1\,, \tag{3.4}$$

for IG and

$$\frac{\delta G_N}{G_N}(z = 0) = \xi\frac{\sigma_{\rm ini}^2 - \sigma_0^2}{N_{\rm pl}^2 + \xi\sigma_0^2} = \frac{\sigma_0^2 - \sigma_{\rm ini}^2}{6N_{\rm pl}^2 - \sigma_0^2} \leq 0\,, \tag{3.5}$$

$$\frac{\dot{G}_N}{G_N}(z = 0) = -\frac{2\xi\dot{\sigma}_0\sigma_0}{N_{\rm pl}^2 + \xi\sigma_0^2} = \frac{2\dot{\sigma}_0\sigma_0}{6N_{\rm pl}^2 - \sigma_0^2} \leq 0\,, \tag{3.6}$$

$$\frac{G_N}{G}(z = 0) = \frac{1}{4}\left(3 + \frac{M_{\rm pl}^2}{N_{\rm pl}^2}\right) \leq 1\,, \tag{3.7}$$

for the CC case, where $\delta G_N/G_N$, $\dot{G}_N/G_N = 0$ and $G_N/G = 1$ correspond to the predictions in GR.

We also list the $\Delta\chi^2 \equiv \chi^2 - \chi^2_{\Lambda CDM}$, where negative values indicate a better-fit to the datasets with respect to the ΛCDM model.

3.1 Datasets

We constrain the cosmological parameters using several combination of datasets. Our CMB measurements are those from the *Planck* 2018 legacy release (hereafter P18) on temperature, polarization, and weak lensing CMB anisotropies angular power spectra [114, 115]. The high-multipoles likelihood $\ell \geq 30$ is based on `Plik` likelihood. We use the low-ℓ likelihood combination at $2 \leq \ell < 30$: temperature-only `Commander` likelihood plus the `SimAll` EE-only likelihood. For the *Planck* CMB lensing likelihood, we consider the *conservative* multipoles range, i.e. $8 \leq \ell \leq 400$. We marginalize over foreground and calibration nuisance parameters of the *Planck* likelihoods [114, 115] which are also varied together with the cosmological ones.

Baryon acoustic oscillation (BAO) measurements from galaxy redshift surveys are used as primary astrophysical dataset to constraint these class of theories providing a complementary late-time information to the CMB anisotropies. We use the Baryon Spectroscopic
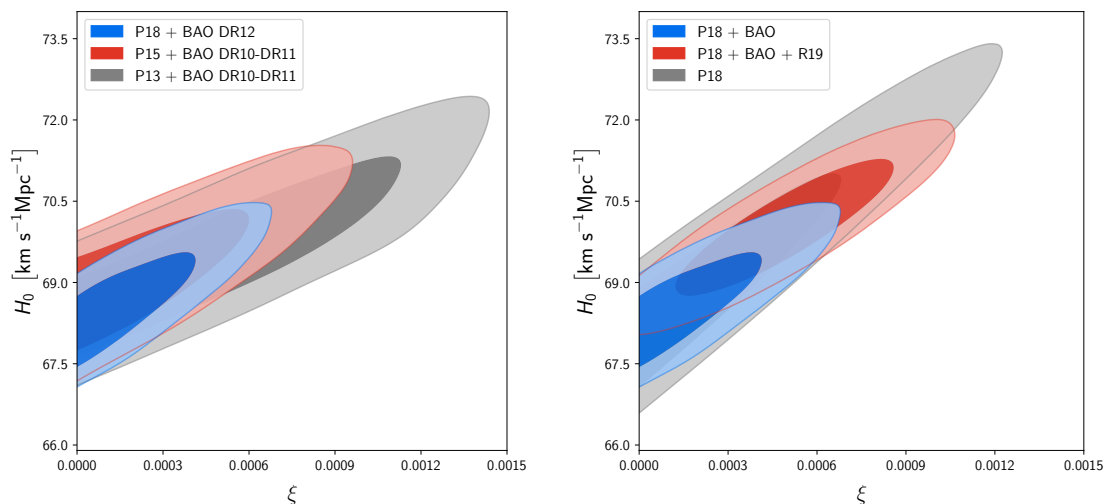
Figure 1. Left panel: marginalized joint 68% and 95% CL regions 2D parameter space using current versus previous releases of *Planck* data and BOSS BAO data from [62, 63]. Right panel: marginalized joint 68% and 95% CL regions 2D parameter space using P18 (gray) in combination with BAO (blue) and BAO + R19 (red) for the IG model.

Survey (BOSS) DR12 [41] *consensus* results on BAOs in three redshift slices with effective redshifts $z_{\rm eff} = 0.38, 0.51, 0.61$ [116–118], in combination with measure from 6dF [39] at $z_{\rm eff} = 0.106$ and the one from SDSS DR7 [40] at $z_{\rm eff} = 0.15$.

Finally, we consider the combination with a Gaussian likelihood based on the determination of the Hubble constant from Hubble Space Telescope (HST) observations (hereafter R19), i.e. $H_0 = (74.03 \pm 1.42)$ km s^{-1}Mpc^{-1} [8].

4 Updated *Planck* 2018 results

The results in this section update those obtained in ref. [63] for IG and in ref. [66] for CC, based on the *Planck* 2015 data (P15) [119, 120] in combination with an older compilation of BAO data, i.e. DR10-DR11 [39, 40, 122].

First, we discuss the IG case. We find that the constraint on the coupling parameter ξ obtained from the CMB alone is almost half of the bound obtained with P15 which was $\xi < 0.0017$ at 95% CL. With the full high-ℓ polarization information and the new determination of τ we obtain $\xi < 0.00098$ at 95% CL. Adding the BAO data, we obtain $\xi < 0.00055$ at 95% CL, which is 25% tighter compared to the limit obtained with P15 in combination with BAO DR10-11, i.e. $\xi < 0.00075$ and half of the one obtained with P13 in combination with BAO DR10-11, i.e. $\xi < 0.0012$, see the left panel of figure 1. As we can see from table 1, BAO data strongly constrain the model and are useful to break the degeneracy in the $H_0 - \xi$ parameter space.

We now discuss the CC case. The coupling to gravity is constrained to $N_{\rm pl} < 1.000028$ M$_{\rm pl}$ at 95% CL for P18 and $N_{\rm pl} < 1.000018$ M$_{\rm pl}$ at 95% CL in combination with BAO data. These constraints update the ones obtained with P15 in combination with D10-DR11 BAO $N_{\rm pl} < 1.000038$ M$_{\rm pl}$ at 95% CL in ref. [66]. As in the IG case, we still have a degeneracy between H_0 and the coupling to gravity $N_{\rm pl}$ as visible from figure 2. For these NMC models we recover the same cosmological parameters and uncertainties if we allow ξ
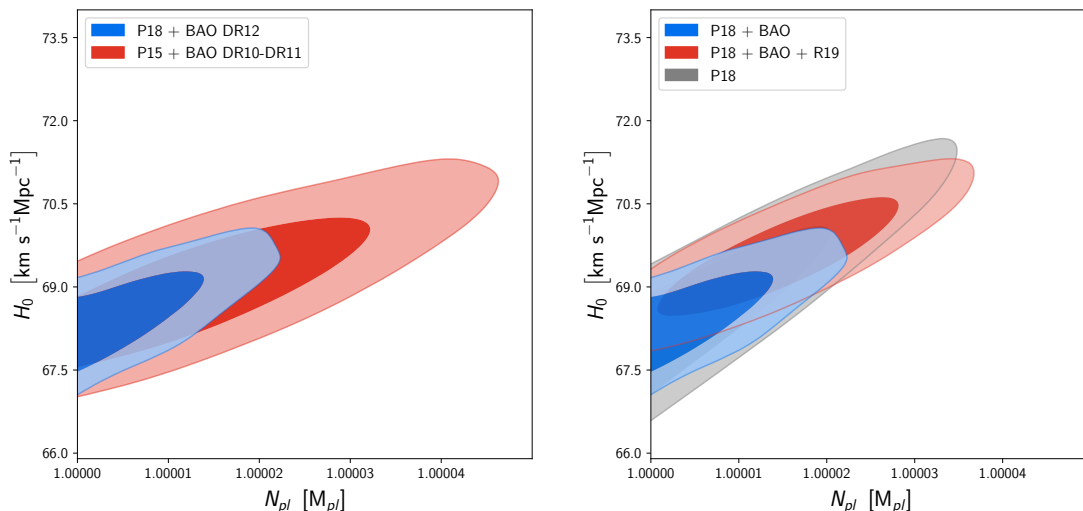
Figure 2. Left panel: marginalized joint 68% and 95% CL regions 2D parameter space using P18 (P15) data in combination BAO in blue (red). Right panel: marginalized joint 68% and 95% CL regions 2D parameter space using P18 (gray) in combination with BAO (blue) and BAO + R19 (red) for the CC model.

to vary, with prior range $[0, 0.1]$ and $[-0.1, 0]$, together with $N_{\rm pl}$. We find for the positive branch ($N_{\rm pl} < M_{\rm pl}$, $\xi > 0$) of the coupling:

$$N_{\rm pl} > 0.64 \; {\rm M_{pl}} \; (> 0.60 \; {\rm M_{pl}}) \,, \qquad \xi < 0.046 \; (< 0.055) \tag{4.1}$$

both at 95% CL and $H_0 = \left(68.78^{+0.56}_{-0.84}\right)$ km s^{-1}Mpc^{-1} $\left(70.14^{+0.86}_{-0.72}\right.$ km s^{-1}Mpc^{-1}) with P18+BAO (P18+BAO+R19). The constraints for the negative branch ($N_{\rm pl} > M_{\rm pl}$, $\xi < 0$) are:

$$N_{\rm pl} < 1.05 \; {\rm M_{pl}} \; (< 1.04 \; {\rm M_{pl}}) \,, \qquad \xi > -0.042 \; (> -0.051) \tag{4.2}$$

both at 95% CL and $H_0 = \left(68.76^{+0.54}_{-0.78}\right)$ km s^{-1}Mpc^{-1} (69.74 ± 0.75 km s^{-1}Mpc^{-1}) with P18+BAO (P18+BAO+R19).

Consistently with the constraints on the coupling parameters ξ and $N_{\rm pl}$, we find also tighter limits on the variation of the Newton's gravitational constant (3.2)–(3.5) and its derivative (3.3)–(3.6) at present time. For IG, we have:

$$\frac{\delta G_{\rm N}}{G_{\rm N}}(z = 0) > -0.016 \,, \qquad \frac{\dot{G}_{\rm N}}{G_{\rm N}}(z = 0) > -0.66 \times 10^{-13} \; {\rm yr}^{-1} \tag{4.3}$$

for P18 + BAO at 95% CL, updating those obtained in ref. [63] with P15 + BAO DR10-11, i.e.

$$\frac{\delta G_{\rm N}}{G_{\rm N}}(z = 0) > -0.027 \,, \qquad \frac{\dot{G}_{\rm N}}{G_{\rm N}}(z = 0) > -1.4 \times 10^{-13} \; {\rm yr}^{-1} \,. \tag{4.4}$$

For CC, we obtain the following 95% CL bounds for P18 + BAO:

$$\frac{\delta G_{\rm N}}{G_{\rm N}}(z = 0) > -0.017 \,, \qquad \frac{\dot{G}_{\rm N}}{G_{\rm N}}(z = 0) > -0.25 \times 10^{-23} \; {\rm yr}^{-1} \,. \tag{4.5}$$

Note that whereas the constraints on $\delta G_{\rm N}/G_{\rm N}(z = 0)$ hardly change for different coupling $F(\sigma)$, the limits on $\dot{G}_{\rm N}/G_{\rm N}(z = 0)$ strongly depend on the details of the model,[11] but are

---

[11]The same behaviour of the constraints on the variation of the Newton's constant and its derivative has been observed changing the potential $V(\sigma)$ for IG, see ref. [63].
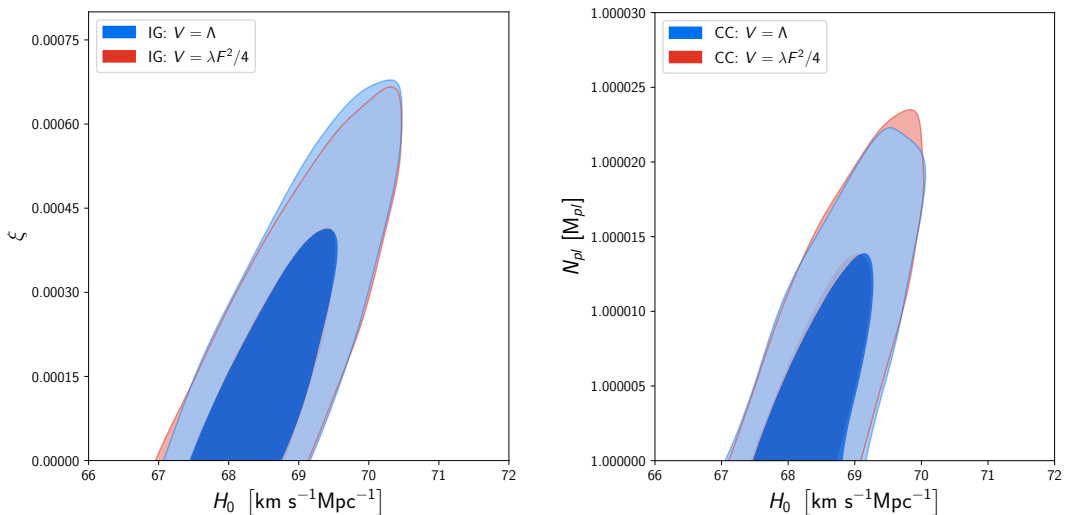
Figure 3. Left panel: marginalized joint 68% and 95% CL regions 2D parameter space $H_0 - \xi$ using P18 + BAO data for IG with $V(\sigma) = \lambda F(\sigma)^2/4$ (red) and $V(\sigma) = \Lambda$ (blue). Right panel: marginalized joint 68% and 95% CL regions 2D parameter space $H_0 - N_{\rm pl}$ using P18 + BAO data for CC with $V(\sigma) = \lambda F(\sigma)^2/4$ (red) and $V(\sigma) = \Lambda$ (blue).

anyway much tighter than those obtained by the Lunar Laser Ranging experiment [121]. Table 1 also reports the values of the post-Newtonian parameters as derived parameters from our samples: whereas for IG $\gamma_{\rm PN} \lesssim \mathcal{O}(10^{-3})$, for CC the bounds we derive on $\gamma_{\rm PN}$, $\beta_{\rm PN}$ are now tighter than those in the Solar System.

We note that the value of the initial (final) scalar field is small and sub-Planckian $\sigma_{ini} = (0.22 \pm 0.10)$ $M_{\rm pl}$ $(\sigma_0 = (0.0089 \pm 0.0040)$ $M_{\rm pl})$ as opposed to the IG case where the evolution is super-Planckian.

We have tested that our results are stable when we switch to a flat potential $V(\sigma) = \Lambda$ for both IG and CC. We show in figure 3 the consistency of the posterior distributions for H_0, ξ, and $N_{\rm pl}$ with current cosmological data (P18 + BAO). The comparison with $V(\sigma) = \Lambda$ for IG updates the results obtained in [63] with *Planck* 2015 which showed that the cosmological parameters were stable when varying the index n of a power-law potential $V(\sigma) = \lambda \sigma^n/4$ with $n \geq 0$. The stability of the results for the CC case when switching to $V(\sigma) = \Lambda$ is a new result, although, in analogy with what happens in IG, not totally unexpected since our data constrains the deviations $\mathcal{O}(\sigma^2/N_{\rm pl}^2)$ of F^2 from a flat potential. We refer the interested reader to ref. [71] for an extended analysis of $V(\sigma) = \Lambda$ for $F(\sigma) = M_{\rm pl}^2 [1 + \xi(\sigma/M_{\rm pl})^n]$ with $n = 2, 4$ with flat priors on $\sigma_{\rm ini}$.[12]

5 Implications for the H_0 tension and combination with R19 data

We find a higher value for the Hubble parameter for IG, i.e. $H_0 = \left(69.6^{+0.8}_{-1.7}\right)$ km s^{-1}Mpc^{-1}, and for CC, i.e. $H_0 = \left(69.0^{+0.7}_{-1.2}\right)$ km s^{-1}Mpc^{-1}, compared to the ΛCDM case, i.e. $H_0 = (67.36 \pm 0.54)$ km s^{-1}Mpc^{-1}, for P18.

The addition of BAO drives the value for H_0 to lower values, for IG to $H_0 = \left(68.78^{+0.53}_{-0.78}\right)$ km s^{-1}Mpc^{-1} and for CC to $H_0 = \left(68.62^{+0.47}_{-0.66}\right)$ km s^{-1}Mpc^{-1}. Note however that these values are larger than the corresponding ΛCDM value, i.e. $H_0 = (67.66 \pm 0.42)$ km s^{-1}Mpc^{-1}.

---

[12]See also ref. [70] for similar finding in NMC scalar-tensor gravity with a coupling $F(\sigma) = M_{\rm pl}^2 + \xi\sigma^2$ in the parameter space range for $\xi < 0$.
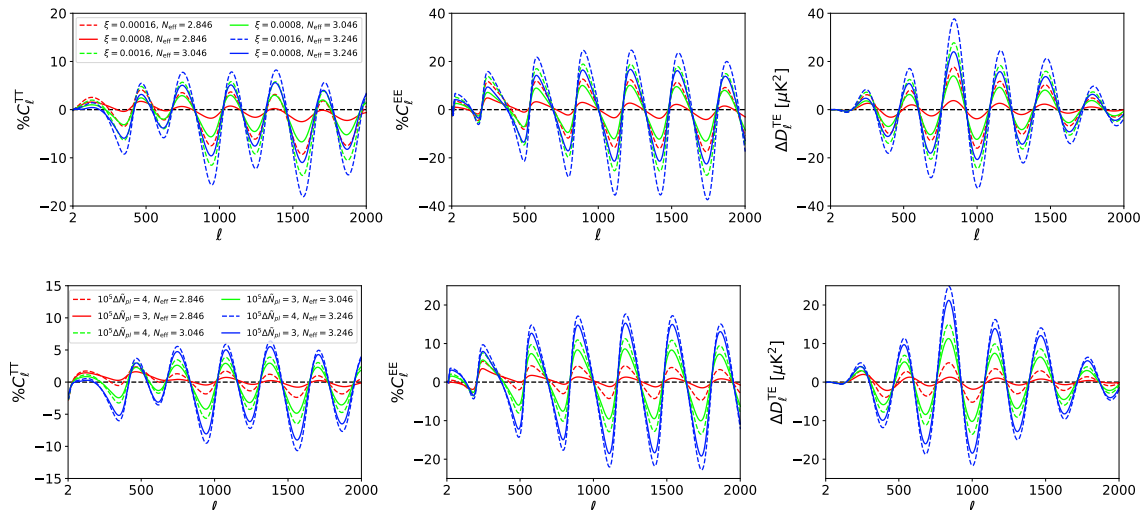
Figure 4. Differences with respect to the ΛCDM with ($N_{\rm eff} = 3.046$) with IG (top panels) for $\xi = 0.0008, 0.0016$ (solid, dashed) and $N_{\rm eff} = 2.846, 3.046, 3.246$ (red, green, blue), and CC (bottom panels) for $N_{\rm pl} = 1.00003, 1.00004$ $M_{\rm pl}$ (solid, dashed) and $N_{\rm eff} = 2.846, 3.046, 3.246$ (red, green, blue). $D_\ell \equiv \ell(\ell+1)C_\ell/(2\pi)$ are the band-power angular power spectra.

Once we include R19, we obtain $H_0 = (70.1 \pm 0.8)$ km s^{-1}Mpc^{-1} at 68% CL, $\xi = 0.00051^{+0.00043}_{-0.00046}$ at 95% CL for IG, $H_0 = \left(69.64^{+0.65}_{-0.73}\right)$ km s^{-1}Mpc^{-1} at 68% CL, $N_{\rm pl} < 1.000031$ $M_{\rm pl}$ at 95% CL for CC. Figure 1 shows how the degeneracy between H_0 and ξ can easily accommodate for larger H_0 value with respect to the ΛCDM concordance model reducing the H_0 *tension* from 4.4σ to 2.7σ (3.2σ) for P18 and 3.5σ (3.6σ) including BAO for IG (CC). The reduction of the tension is due to the combination of having an higher mean and larger uncertainties on H_0 compared to the ΛCDM model. We find that H_0 is about ~ 0.5 km s^{-1}Mpc^{-1} higher in the IG compared to the CC case for every choice of datasets combination.

Note that the models considered in our paper can produce a values of H_0 in complete agreement with the local value of H_0 measured using red giants [16], though not that measured using SNe Ia [8].

6 Degeneracy with the neutrino sector

6.1 Effective number of relativistic degrees of freedom

The presence of extra relativistic degrees of freedom in the Universe increases the expansion rate during the radiation-dominated era and shifts the epoch of matter-radiation equality, the shape of the matter power spectrum, and the history of recombination (see refs. [123, 124] for a review). The extra radiation is usually parameterized by $\Delta N_{\rm eff} \equiv N_{\rm eff} - 3.046$ which takes into account that neutrino decoupling was not quite complete when e^+e^- annihilation began [125–128].

In the context of the H_0 *tension*, a larger value of $N_{\rm eff}$ can attenuate the discrepancy on the H_0 value and reduce the comoving sound horizon at baryon drag. However, the tension is only reduced ($\sim 2\sigma$) and it appears again when BAO data is included [7, 43].

There is an interplay (negative correlation) between the contribution of extra radiation with respect to the standard ΛCDM scenario from the $N_{\rm eff}$ and from the scalar field cou-
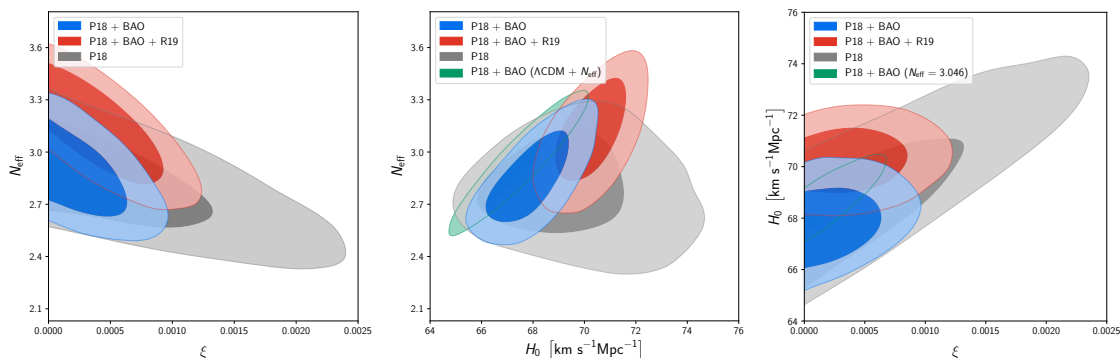
Figure 5. Marginalized joint 68% and 95% CL regions 2D parameter space using the P18 (gray) in combination with BAO (blue) and BAO + R19 (red) for the IG+$N_{\rm eff}$ model. In the central panel, we include the $H_0 - N_{\rm eff}$ contours for the ΛCDM in green. In the right panel, we include the $H_0 - \xi$ contours for the IG with $N_{\rm eff} = 3.046$ in green.
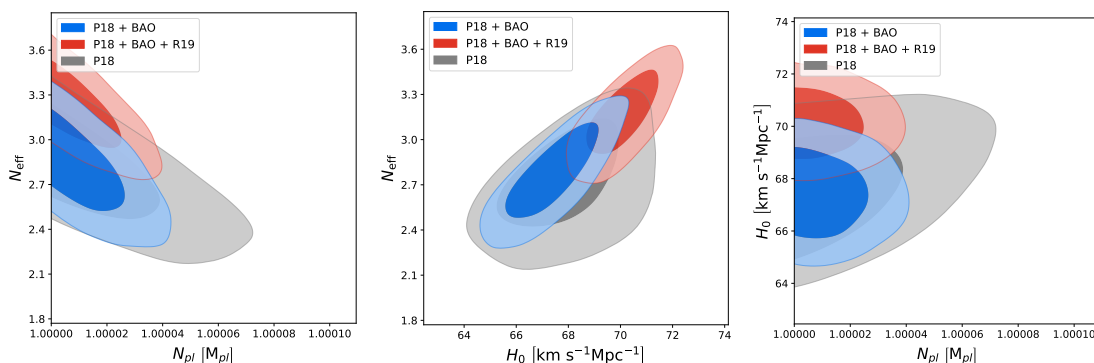
Figure 6. Marginalized joint 68% and 95% CL regions 2D parameter space using the *Planck* legacy data (gray) in combination with DR12 (blue) and DR12 + R19 (red) for the CC+$N_{\rm eff}$ model.

pling[13] which acts as an additional source of radiation in the early Universe. Decreasing the effective number of extra relativistic species to $N_{\rm eff} = 2.846$ we obtain deviations of the CMB anisotropies angular power spectra to the ΛCDM model of the same order of the ones obtained with ξ halved and $N_{\rm eff} = 3.046$, see figure 4.

We see that, preferring lower values of $N_{\rm eff}$, the dataset allows for larger values for ξ compared to the case with $N_{\rm eff} = 3.046$ fixed. We go from $\xi < 0.00098$ to $\xi < 0.0019$ at 95% CL with P18 alone and from $\xi < 0.00055$ to $\xi < 0.00078$ once we include BAO, see table 3.

The mean of $N_{\rm eff}$ moves around 1σ toward lower values with respect to the ΛCDM case with a similar error. For IG, we get at 68% CL $N_{\rm eff} = 2.79 \pm 0.20$ for P18 compared to $N_{\rm eff} = 2.89 \pm 0.19$ in ΛCDM and $N_{\rm eff} = 2.85 \pm 0.17$ in combination with BAO compared to $N_{\rm eff} = 2.99 \pm 0.17$ in ΛCDM. In figure 5 (central panel), we show the enlarged $H_0 - N_{\rm eff}$ parameter space in IG compared to the ΛCDM concordance model (green contours) where it is possible to reach higher value of H_0 without increasing $N_{\rm eff}$ in presence of a modification of gravity.

In the CC model, an analogous correlation in the $N_{\rm eff} - N_{\rm pl}$ parameter space is found, see figure 6. The constraints on $N_{\rm pl}$ are larger, from $N_{\rm pl} < 1.000028$ M$_{\rm pl}$ to $N_{\rm pl} < 1.000057$

---

[13]See refs. [72, 73] for an application in the context of $f(R)$ gravity.

M_{pl} at 95% CL with P18 alone and from $N_{pl} < 1.000018$ M_{pl} to $N_{pl} < 1.000019$ M_{pl} at 95% CL once we include BAO, see table 4.

While for the combination P18 + BAO we find a higher value for the Hubble parameter for IG, i.e. $H_0 = \left(68.78^{+0.53}_{-0.78}\right)$ km s^{-1}Mpc^{-1}, and for CC, i.e. $H_0 = \left(68.62^{+0.47}_{-0.66}\right)$ km s^{-1}Mpc^{-1}, compared to the ΛCDM+N_{eff} case, i.e. $H_0 = (67.3 \pm 1.1)$ km s^{-1}Mpc^{-1}, the addition of R19 data leads to a closer posterior distribution for H_0 among the three cases, i.e. (70.1 ± 0.8) km s^{-1}Mpc^{-1} for IG, (69.6 ± 0.7) km s^{-1}Mpc^{-1} for CC, and $H_0 = (70.0 \pm 0.9)$ km s^{-1}Mpc^{-1} for ΛCDM+N_{eff}. We find a similar posterior distribution also for IG+N_{eff} (CC+N_{eff}), i.e. (70.3 ± 0.9) km s^{-1}Mpc^{-1} $((70.1 \pm 0.9)$ km s^{-1}Mpc$^{-1})$, see figure 5.

The addition of BAO data reduces the degeneracy $H_0 - \xi$ $(-N_{pl})$ increasing the one between $N_{eff} - \xi$ $(-N_{pl})$ and $H_0 - N_{eff}$. In order to reduce comoving sound horizon to accommodate a larger value of H_0, in this case N_{eff} is moved towards larger values, i.e. 3.11 ± 0.19 for IG and 3.16 ± 0.19 for CC, see table 3.

6.2 Neutrino mass

The changes in the background evolution caused by neutrino mass, under standard assumptions and for a fixed set of standard cosmological parameters, are confined to late times. In particular, the neutrino mass impact the angular diameter distance and z_Λ (the redshift of matter-to-cosmological-constant equality) (see refs. [123, 124, 129–133] for a review on neutrino mass in cosmology).

In the standard ΛCDM scenario, a larger value of m_ν results in a lower Hubble rate inferred from the CMB, exacerbating the H_0 *tension*. However, there is partial correlation between the equation of state of dark energy (DE) w and the total neutrino mass m_ν, as first noticed by [130]. When m_ν is increased (or more generally Ω_ν), Ω_m can be kept unchanged, by simultaneously decreasing w, in order to keep the angular diameter distance at decoupling fixed. In this case, the impact of neutrino mass on the background is confined to variations of z_Λ and of the late-time ISW effect.

Cosmological bounds on the neutrino masses can therefore be relaxed by using a DE component rather than a cosmological constant. Vice versa, cosmological constraints on the DE parameters become larger in comparison to cosmologies with massless neutrinos or with the standard minimal assumption of $m_\nu = 0.06$ eV. The same conclusions have been obtained in the context of Galileon gravity [76].

We show in figure 7 the combined effect on the CMB anisotropies of varying both ξ and m_ν in the IG model. For a fixed value of the coupling parameter $\xi = 0.0008$, the differences with respect to the ΛCDM concordance model are reduced by increasing the value of the neutrino mass m_ν from 0.1 eV to 0.3 eV. On the late-time observables, i.e. the weak lensing CMB anisotropies and the linear matter power spectrum, the partial degeneracy between modified gravity and the neutrino mass is still present but with differences concentrated on small scales, see figure 8.

In this case the constraints on the coupling parameter ξ become tighter compared to the case with $m_\nu = 0$, i.e. from $\xi < 0.00098$ to $\xi < 0.00094$ at 95% CL for P18.[14] The CMB anisotropies data prefer to relax the upper bound on the neutrino mass which becomes $m_\nu < 0.31$ eV at 95% CL for P18 29% larger to the ΛCDM case $m_\nu < 0.24$ eV. Including the BAO data, the total neutrino mass is constrained to $m_\nu < 0.17$ eV at 95% CL, 42% larger to the ΛCDM case $m_\nu < 0.12$ eV, and we find $\xi < 0.00076$ at 95% CL, see table 5. The

---

[14]We assume one massive and two massless neutrinos.
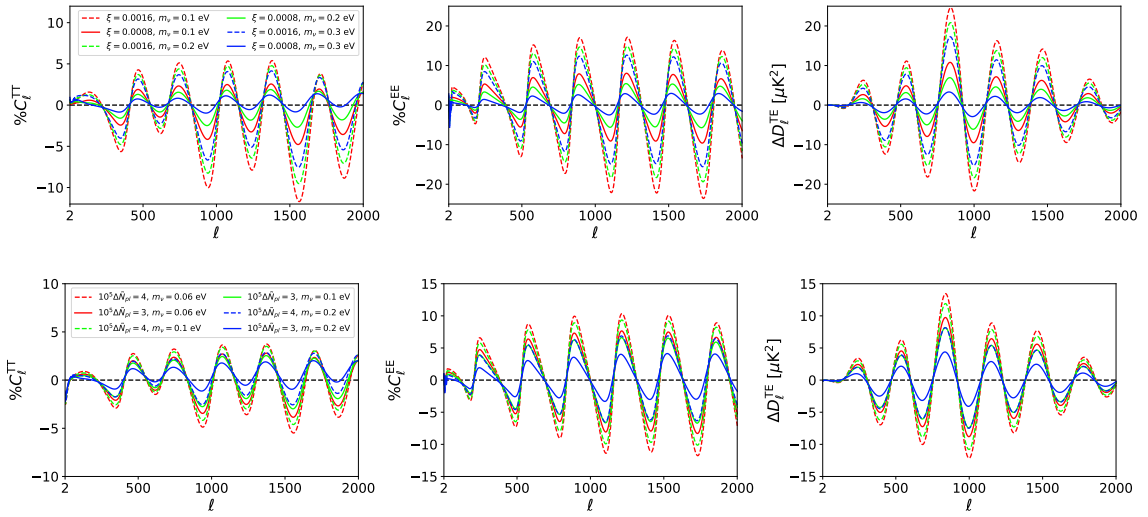
Figure 7. Differences with respect to the ΛCDM with $m_\nu = 0\,\text{eV}$ with IG (top panels) for $\xi = 0.0008, 0.0016$ (solid, dashed) and $m_\nu = 0.1, 0.2, 0.3\,\text{eV}$ (red, green, blue), and CC (bottom panels) for $N_{\text{pl}} = 1.00003, 1.00004\,\text{M}_{\text{pl}}$ (solid, dashed) and $m_\nu = 0.06, 0.1, 0.2\,\text{eV}$ (red, green, blue).
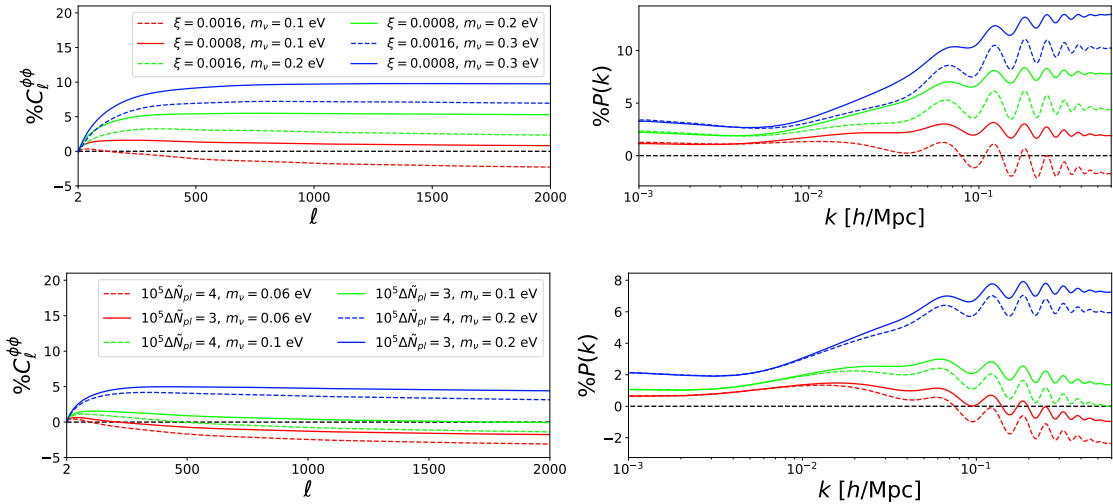
Figure 8. Differences with respect to the ΛCDM with $m_\nu = 0\,\text{eV}$ with IG (top panels) for $\xi = 0.0008, 0.0016$ (solid, dashed) and $m_\nu = 0.1, 0.2, 0.3\,\text{eV}$ (red, green, blue), and CC (bottom panels) for $N_{\text{pl}} = 1.00003, 1.00004\,\text{M}_{\text{pl}}$ (solid, dashed) and $m_\nu = 0.06, 0.1, 0.2\,\text{eV}$ (red, green, blue).

addition of R19 data leads to $H_0 = (70.1 \pm 0.8)$ km s^{-1}Mpc^{-1} with an upper bound on the total neutrino mass $m_\nu < 0.19\,\text{eV}$ at 95% CL, 2.5 times larger than the limit based on the ΛCDM model, with a 2σ detection of the coupling parameter $\xi = 0.00065 \pm 0.00057$ at 95% CL, see figure 9.

Analogously, for CC the constraint on N_{pl} becomes tighter compared to the case with $m_\nu = 0$, i.e. $N_{\text{pl}} < 1.000026\,\text{M}_{\text{pl}}$ for P18 and $N_{\text{pl}} < 1.000024\,\text{M}_{\text{pl}}$ for P18 + BAO at 95% CL, see figure 10. Also, for this model, the upper bound on the neutrino mass becomes 30% larger compared to the ΛCDM case, see table 6.
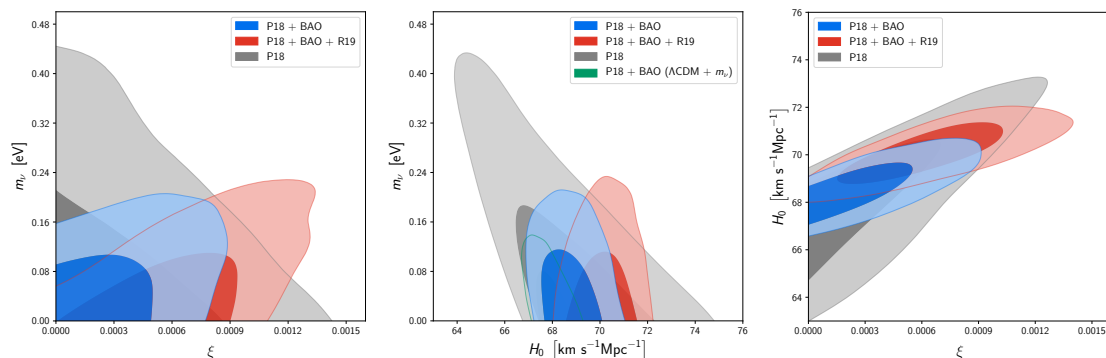
Figure 9. Marginalized joint 68% and 95% CL regions 2D parameter space using P18 (gray) in combination with BAO (blue) and BAO + R19 (red) for the IG+m_ν model. In the central panel, we include the $H_0 - N_{\rm eff}$ contours for the ΛCDM in green.
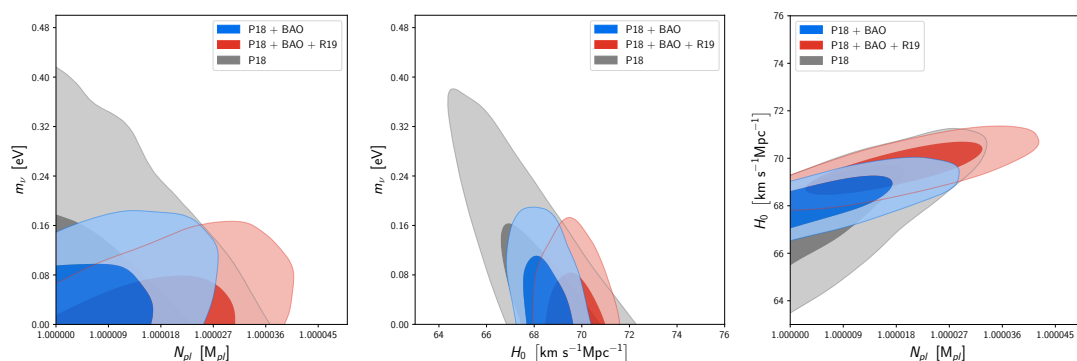
Figure 10. Marginalized joint 68% and 95% CL regions 2D parameter space using P18 (gray) in combination with BAO (blue) and BAO + R19 (red) for the CC+m_ν model.

6.3 Joint constraints on $N_{\rm eff}$ and neutrino mass

Finally, we consider the case where both $N_{\rm eff}$ and m_ν are allowed to vary. Despite the larger parameter space and the larger limits on the parameters, the models do not accommodate higher values of the Hubble parameter compared to the 7- and 8-parameters case analysed before, see figures 11–12. Moreover, the total neutrino mass is almost uncorrelated with the Hubble parameter. In this case, the modified gravity parameters ξ and $N_{\rm pl}$ are always compatible at 2σ with the GR limit due to the larger parameter space and are given by (see tables 7–8):

$$\xi < 0.0018 \ (95\% \ {\rm CL}) \,, \qquad N_{\rm eff} = 2.74 \pm 0.22 \,, \qquad m_\nu < 0.26 \ {\rm eV} \ (95\% \ {\rm CL})$$

for IG and

$$N_{\rm pl} < 1.000050 \ {\rm M_{pl}} \ (95\% \ {\rm CL}) \,, \qquad N_{\rm eff} = 2.73 \pm 0.21 \,, \qquad m_\nu < 0.26 \ {\rm eV} \ (95\% \ {\rm CL})$$

for the CC case. When we include BAO data, we obtain

$$\xi < 0.0012 \ (95\% \ {\rm CL}) \,, \qquad N_{\rm eff} = 2.77 \pm 0.20 \,, \qquad m_\nu < 0.19 \ {\rm eV} \ (95\% \ {\rm CL})$$

for IG and

$$N_{\rm pl} < 1.000042 \ {\rm M_{pl}} \ (95\% \ {\rm CL}) \,, \qquad N_{\rm eff} = 2.75 \pm 0.21 \,, \qquad m_\nu < 0.17 \ {\rm eV} \ (95\% \ {\rm CL})$$
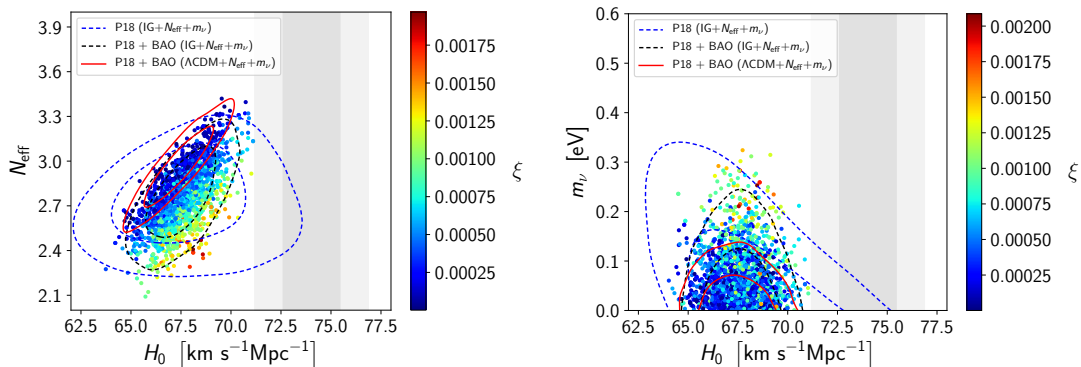
Figure 11. Samples of the P18 + BAO chains in the $H_0 - N_{\mathrm{eff}}$ ($H_0 - m_\nu$) plane, colour-coded by ξ for the IG+N_{eff}+m_ν model. Dashed blue contours show the constraints for IG+N_{eff}+m_ν with P18 alone. Solid red contours show the constraints for the ΛCDM+N_{eff}+m_ν model. The gray bands denote the local Hubble parameter measurement from R19 [8].
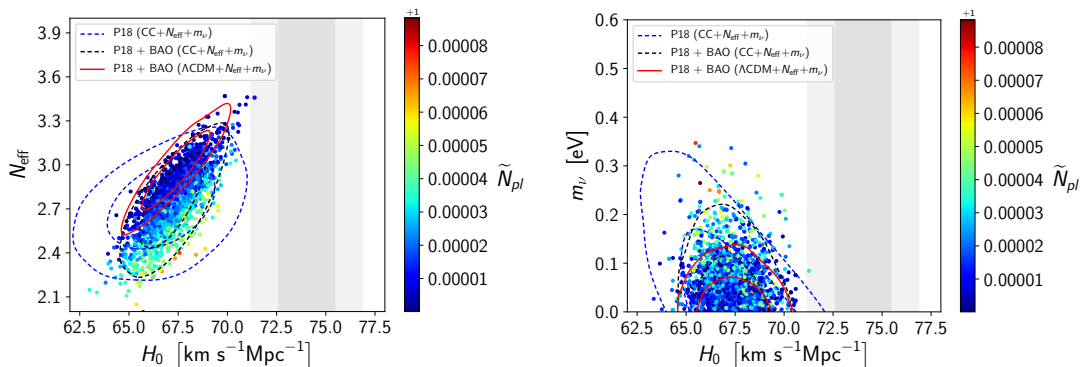
Figure 12. Samples of the P18 + BAO chains in the $H_0 - N_{\mathrm{eff}}$ ($H_0 - m_\nu$) plane, colour-coded by N_{pl} for the CC+N_{eff}+m_ν model. Dashed blue contours show the constraints for CC+N_{eff}+m_ν with P18 alone. Solid red contours show the constraints for the ΛCDM+N_{eff}+m_ν model. The gray bands denote the local Hubble parameter measurement from R19 [8].

for the CC case. Adding also R19, we obtain

$$\xi < 0.0013 \ (95\% \ \mathrm{CL}), \qquad N_{\mathrm{eff}} = 3.08 \pm 0.20, \qquad m_\nu < 0.19 \ \mathrm{eV} \ (95\% \ \mathrm{CL})$$

for IG and

$$N_{\mathrm{pl}} < 1.000040 \ \mathrm{M_{pl}} \ (95\% \ \mathrm{CL}), \qquad N_{\mathrm{eff}} = 3.14 \pm 0.20, \qquad m_\nu < 0.14 \ \mathrm{eV} \ (95\% \ \mathrm{CL})$$

for the CC case.

7 Conclusions

We have studied the simplest class of scalar-tensor theories of gravity where Newton's constant is allowed to vary in time and space. These non-minimally coupled theories are characterized by a coupling to the Ricci scalar R of the type $F(\sigma) = N_{\mathrm{pl}}^2 + \xi \sigma^2$, which contain the *induced gravity* [138–140] model for $N_{\mathrm{pl}} = 0$ and $\xi > 0$, and the *conformal coupling* model [66] for $\xi = -1/6$. These models contribute to the radiation density budget in the

radiation-dominated epoch and change the background expansion history compared to the ΛCDM concordance model naturally alleviating the H_0 *tension*.

Compared to previous constraints [63, 66], the improvement of *Planck* 2018 polarization data lead to tighter results, i.e. $\xi < 0.00098$ and $N_{\rm pl} < 1.000028$ M$_{\rm pl}$ both at 95% CL. When BAO data from BOSS DR12 are added, we obtain tighter limits, i.e. $\xi < 0.00055$ and $N_{\rm pl} < 1.000018$ M$_{\rm pl}$. For $\xi = -1/6$, P18 and BAO data lead to constraints on the post-Newtonian parameters which are tighter than those derived within the Solar System.

It is interesting to note that for CMB and BAO data these models allow for values of H_0 larger than ΛCDM. Using P18 data, we find $H_0 = \left(69.6^{+0.8}_{-1.7}\right)$ km s^{-1}Mpc^{-1} ($H_0 = \left(69.0^{+0.7}_{-1.2}\right)$ km s^{-1}Mpc^{-1}) for the IG (CC) case compared to $H_0 = (67.36 \pm 0.54)$ km s^{-1}Mpc^{-1} for ΛCDM, alleviating the tension from 4.4σ to 2.7σ (3.2σ) for P18 and 3.5σ (3.6σ) including BAO for IG (CC).

Including BAO and R19, we obtain $H_0 = (70.06 \pm 0.81)$ km s^{-1}Mpc^{-1} ($H_0 = \left(69.64^{+0.65}_{-0.73}\right)$ km s^{-1}Mpc^{-1}) for IG (for CC). The value for H_0 we find is similar to what can be obtained in other models which aim to solve the H_0 tension, but the models considered here have just one extra parameter as ΛCDM+$N_{\rm eff}$. Similar valus of H_0 can also be found for NMC beyond the IG and CC cases considered here [71].

We have extended our analysis to a general neutrino sector by allowing the effective number of relativistic species $N_{\rm eff}$ and the neutrino mass m_ν to vary. Both $N_{\rm eff}$ and m_ν are partially degenerate with the deviations from GR, as happens in other modified gravity models [72, 73, 76]. Whereas $N_{\rm eff}$ and the scalar field act as an additional source of radiation in the early Universe, at late times the background contribution to Ω_m due to m_ν can be compensated from the scalar field in order to keep the angular diameter distance at decoupling fixed, see figures 4–7–8. We have shown however that these are only partial degeneracies which could be broken by combination of observations at different redshifts.

In case with $N_{\rm eff}$ (section 6.1) the limit on ξ becomes $\sim 94\%$ ($\sim 42\%$) larger with P18 (P18+BAO) while the mean on the number of neutrinos moves around 1σ towards lower values compared to the ΛCDM case without significantly degrading its uncertainty, i.e. $N_{\rm eff} = 2.79 \pm 0.20$ ($N_{\rm eff} = 2.85 \pm 0.17$). For CC the limit on $N_{\rm pl}$ becomes $\sim 104\%$ ($\sim 6\%$) larger with P18 (P18+BAO) and analogously to IG we find $N_{\rm eff} = 2.73^{+0.25}_{-0.22}$ ($N_{\rm eff} = 2.81 \pm 0.19$).

The upper bound on the neutrino mass (section 6.2) is $\sim 29\%$ ($\sim 42\%$) is also degraded with P18 (P18+BAO) compared to the ΛCDM case, i.e. $m_\nu < 0.31$ eV ($m_\nu < 0.17$ eV), whereas the constraint on ξ is slightly tighter with CMB data alone in order to relax the constraint on m_ν. Analogously, for CC the limit on the neutrino mass is $\sim 17\%$ ($\sim 33\%$) larger with P18 (P18+BAO) compared to the ΛCDM case. When both $N_{\rm eff}$ and m_ν are allowed to vary, we see that the constraints on ξ and $N_{\rm pl}$ degrade by a factor two compared to the case with $N_{\rm eff} = 3.046$ and $m_\nu = 0$ eV also in presence of BAO data, i.e. $\xi < 0.0012$ and $N_{\rm pl} < 1.000042$ M$_{\rm pl}$ at 95% CL. For the data used, the combination of the modification to gravity in our models to non-standard neutrino physics does not lead to higher values of H_0 compared to the case with standard assumptions in the neutrino sector.

Acknowledgments

A Tables

A.1 Updated *Planck* 2018 results

	P18	P18 + BAO	P18 + BAO + R19
ω_{b}	$0.02244^{+0.00014}_{-0.00016}$	0.02239 ± 0.00013	0.02246 ± 0.00013
ω_{c}	0.1198 ± 0.0012	0.1201 ± 0.0011	0.1200 ± 0.0011
H_0 [km s^{-1}Mpc^{-1}]	$69.6^{+0.8}_{-1.7}$ (2.7σ)	$68.78^{+0.53}_{-0.78}$ (3.5σ)	70.06 ± 0.81 (2.4σ)
τ	$0.0551^{+0.0065}_{-0.0078}$	$0.0545^{+0.0063}_{-0.0071}$	$0.0554^{+0.0064}_{-0.0073}$
$\ln\left(10^{10}A_{\mathrm{s}}\right)$	$3.047^{+0.014}_{-0.015}$	3.046 ± 0.013	3.049 ± 0.013
n_{s}	$0.9680^{+0.0044}_{-0.0052}$	0.9662 ± 0.0038	0.9688 ± 0.0037
ζ_{IG}	< 0.0039 (95% CL)	< 0.0022 (95% CL)	$0.00202^{+0.00090}_{-0.00100}$
ξ	< 0.00098 (95% CL)	< 0.00055 (95% CL)	$0.00051^{+0.00043}_{-0.00046}$ (95% CL)
γ_{PN}	> 0.9961 (95% CL)	> 0.9978 (95% CL)	$0.9980^{+0.0010}_{-0.0009}$
$\delta G_{\mathrm{N}}/G_{\mathrm{N}}$ (z=0)	> -0.029 (95% CL)	> -0.016 (95% CL)	-0.0149 ± 0.0068
$10^{13}\dot{G}_{\mathrm{N}}/G_{\mathrm{N}}$ (z=0) [yr^{-1}]	> -1.16 (95% CL)	> -0.66 (95% CL)	-0.61 ± 0.28
G_{N}/G (z=0)	> 0.9981 (95% CL)	> 0.9989 (95% CL)	$0.99899^{+0.00050}_{-0.00045}$
Ω_{m}	$0.2940^{+0.0150}_{-0.0095}$	$0.3013^{+0.0072}_{-0.0062}$	0.2903 ± 0.0068
σ_8	$0.8347^{+0.0074}_{-0.0130}$	$0.8308^{+0.0067}_{-0.0096}$	0.840 ± 0.010
r_s [Mpc]	$146.37^{+0.79}_{-0.40}$	$146.63^{+0.55}_{-0.34}$	$146.03^{+0.67}_{-0.59}$
$\Delta\chi^2$	0.2	0.2	-3.1

Table 1. Constraints on main and derived parameters (at 68% CL if not otherwise stated) considering P18 in combination with BAO and BAO + R19 for the IG model.

	P18	P18 + BAO	P18 + BAO + R19
ω_{b}	0.02244 ± 0.00015	0.02241 ± 0.00013	0.0250 ± 0.0013
ω_{c}	0.1197 ± 0.0012	0.11990 ± 0.00094	0.1195 ± 0.0010
H_0 [km s^{-1}Mpc^{-1}]	$69.0^{+0.7}_{-1.2}$ (3.2σ)	$68.62^{+0.47}_{-0.66}$ (3.6σ)	$69.64^{+0.65}_{-0.73}$ (2.8σ)
τ	$0.0554^{+0.0064}_{-0.0081}$	$0.0551^{+0.0058}_{-0.0076}$	$0.0562^{+0.0066}_{-0.0077}$
$\ln\left(10^{10}A_{\mathrm{s}}\right)$	$3.048^{+0.013}_{-0.016}$	$3.047^{+0.011}_{-0.015}$	$3.050^{+0.013}_{-0.015}$
n_{s}	0.9684 ± 0.0047	0.9668 ± 0.0039	0.9707 ± 0.0040
N_{pl} [M$_{\mathrm{pl}}$]	< 1.000028 (95% CL)	< 1.000018 (95% CL)	< 1.000031 (95% CL)
γ_{PN}	> 0.999972 (95% CL)	> 0.999982 (95% CL)	> 0.999969 (95% CL)
β_{PN}	< 1.0000023 (95% CL)	< 1.0000015 (95% CL)	< 1.0000025 (95% CL)
$\delta G_{\mathrm{N}}/G_{\mathrm{N}}$ (z=0)	> -0.026 (95% CL)	> -0.017 (95% CL)	> -0.029 (95% CL)
$10^{13}\dot{G}_{\mathrm{N}}/G_{\mathrm{N}}$ (z=0) [yr^{-1}]	$> -3.8 \times 10^{-9}$ (95% CL)	$> -2.5 \times 10^{-9}$ (95% CL)	$> -4.2 \times 10^{-9}$ (95% CL)
G_{N}/G (z=0)	> 0.999986 (95% CL)	> 0.999991 (95% CL)	> 0.999985 (95% CL)
Ω_{m}	$0.299^{+0.011}_{-0.009}$	0.3023 ± 0.0061	0.2928 ± 0.0064
σ_8	$0.832^{+0.011}_{-0.007}$	$0.8299^{+0.0060}_{-0.0088}$	$0.8364^{+0.0089}_{-0.011}$
r_s [Mpc]	$146.71^{+0.46}_{-0.33}$	$146.82^{+0.37}_{-0.28}$	$146.53^{+0.51}_{-0.42}$
$\Delta\chi^2$	2.2	0.8	-1.7

Table 2. Constraints on main and derived parameters (at 68% CL if not otherwise stated) considering P18 in combination with BAO and BAO + R19 for the CC model.

A.2 Degeneracy with the neutrino sector: N_{eff}

	P18	P18 + BAO	P18 + BAO + R19
ω_{b}	$0.02227^{+0.00018}_{-0.00021}$	0.02225 ± 0.00019	0.02250 ± 0.00019
ω_{c}	0.1161 ± 0.0031	0.1172 ± 0.0030	0.1210 ± 0.0029
H_0 [km s^{-1}Mpc^{-1}]	$69.2^{+1.5}_{-2.4}$ (2.3σ)	$67.9^{+1.0}_{-1.2}$ (3.5σ)	70.28 ± 0.92 (2.2σ)
τ	0.0547 ± 0.0078	0.0526 ± 0.0069	0.0549 ± 0.0072
$\ln\left(10^{10}A_{\text{s}}\right)$	3.038 ± 0.016	3.035 ± 0.015	3.050 ± 0.016
n_{s}	$0.9617^{+0.0049}_{-0.0088}$	$0.9600^{+0.0045}_{-0.0079}$	0.9707 ± 0.0069
ζ_{IG}	< 0.0076 (95% CL)	< 0.0031 (95% CL)	< 0.0040 (95% CL)
N_{eff}	2.79 ± 0.20	2.85 ± 0.17	3.11 ± 0.19
ξ	< 0.0019 (95% CL)	< 0.00078 (95% CL)	< 0.0010 (95% CL)
γ_{PN}	> 0.9925 (95% CL)	> 0.9969 (95% CL)	> 0.9960 (95% CL)
$\delta G_{\text{N}}/G_{\text{N}}$ (z=0)	> -0.055 (95% CL)	> -0.023 (95% CL)	> -0.029 (95% CL)
$10^{13}\dot{G}_{\text{N}}/G_{\text{N}}$ (z=0) [yr^{-1}]	> -2.2 (95% CL)	> -0.93 (95% CL)	> -1.2 (95% CL)
$\delta G_{\text{N}}/G$ (z=0)	> 0.9962 (95% CL)	> 0.9985 (95% CL)	> -0.9980 (95% CL)
Ω_{m}	$0.290^{+0.022}_{-0.012}$	0.3022 ± 0.0074	0.2906 ± 0.0067
σ_8	$0.834^{+0.012}_{-0.018}$	0.825 ± 0.010	0.841 ± 0.010
r_s [Mpc]	$148.2^{+1.8}_{-1.5}$	148.4 ± 1.7	145.5 ± 1.5
$\Delta\chi^2$	1.7	-1.8	-3.0

Table 3. Constraints on main and derived parameters (at 68% CL if not otherwise stated) considering P18 in combination with BAO and BAO + R19 for the IG+N_{eff} model.

	P18	P18 + BAO	P18 + BAO + R19
ω_{b}	0.02223 ± 0.00022	0.02215 ± 0.00022	0.02257 ± 0.00018
ω_{c}	0.1151 ± 0.0033	0.1162 ± 0.0031	0.1213 ± 0.0030
H_0 [km s^{-1}Mpc^{-1}]	67.9 ± 1.4 (3.1σ)	67.1 ± 1.2 (3.7σ)	70.10 ± 0.92 (2.0σ)
τ	$0.0539^{+0.0060}_{-0.0074}$	$0.0544^{+0.0061}_{-0.0074}$	$0.0561^{+0.0063}_{-0.0075}$
$\ln\left(10^{10}A_{\text{s}}\right)$	3.034 ± 0.017	3.035 ± 0.016	$3.053^{+0.014}_{-0.016}$
n_{s}	0.9598 ± 0.0084	0.9606 ± 0.0071	0.9736 ± 0.0062
N_{pl} [M$_{\text{pl}}$]	< 1.000057 (95% CL)	< 1.000019 (95% CL)	< 1.000032 (95% CL)
N_{eff}	$2.73^{+0.25}_{-0.22}$	2.81 ± 0.19	3.16 ± 0.19
γ_{PN}	> 0.999943 (95% CL)	> 0.999981 (95% CL)	> 0.999968 (95% CL)
β_{PN}	< 1.0000048 (95% CL)	< 1.0000015 (95% CL)	< 1.0000027 (95% CL)
$\delta G_{\text{N}}/G_{\text{N}}$ (z=0)	> -0.052 (95% CL)	> -0.018 (95% CL)	> -0.030 (95% CL)
$10^{13}\dot{G}_{\text{N}}/G_{\text{N}}$ (z=0) [yr^{-1}]	$> -7.5 \times 10^{-9}$ (95% CL)	$> -2.5 \times 10^{-9}$ (95% CL)	$> -4.3 \times 10^{-9}$ (95% CL)
G_{N}/G (z=0)	> 0.999975 (95% CL)	> 0.999991 (95% CL)	> 0.999984 (95% CL)
Ω_{m}	$0.299^{+0.014}_{-0.011}$	0.3070 ± 0.0066	0.2929 ± 0.0062
σ_8	$0.827^{+0.011}_{-0.013}$	0.8204 ± 0.0099	0.8391 ± 0.0095
r_s [Mpc]	149.5 ± 2.0	149.3 ± 2.0	145.5 ± 1.6
$\Delta\chi^2$	1.4	-0.2	-3.8

Table 4. Constraints on main and derived parameters (at 68% CL if not otherwise stated) considering P18 in combination with BAO and BAO + R19 for the CC+N_{eff} model.

A.3 Degeneracy with the neutrino sector: m_ν

	P18	P18 + BAO	P18 + BAO + R19
$\omega_{\rm b}$	0.02239 ± 0.00017	0.02241 ± 0.00014	0.02247 ± 0.00013
$\omega_{\rm c}$	0.1205 ± 0.0013	0.1203 ± 0.0011	0.1203 ± 0.0012
H_0 [km s^{-1}Mpc^{-1}]	68.5 ± 1.8 (2.4σ)	$68.66^{+0.69}_{-0.87}$ (3.4σ)	70.12 ± 0.81 (2.4σ)
τ	$0.0567^{+0.0065}_{-0.0082}$	$0.0564^{+0.0066}_{-0.0080}$	$0.0572^{+0.0063}_{-0.0080}$
$\ln\left(10^{10}A_{\rm s}\right)$	$3.052^{-0.016}_{+0.013}$	$3.051^{-0.016}_{+0.013}$	$3.054^{+0.013}_{-0.016}$
$n_{\rm s}$	0.9668 ± 0.0053	0.9672 ± 0.0038	0.9700 ± 0.0038
$\zeta_{\rm IG}$	< 0.0037 (95% CL)	< 0.0030 (95% CL)	$0.0026^{+0.0010}_{-0.0013}$
m_ν [eV]	< 0.31 (95% CL)	< 0.17 (95% CL)	< 0.19 (95% CL)
ξ	< 0.00094 (95% CL)	< 0.00076 (95% CL)	0.00065 ± 0.00057 (95% CL)
γ_{PN}	> 0.9963 (95% CL)	> 0.9970 (95% CL)	$0.9974^{+0.0013}_{-0.0010}$
$\delta G_{\rm N}/G_{\rm N}$ (z=0)	> -0.027 (95% CL)	> -0.022 (95% CL)	$-0.0190^{+0.0093}_{-0.0075}$
$10^{13}\dot{G}_{\rm N}/G_{\rm N}$ (z=0) [yr^{-1}]	> -1.1 (95% CL)	> -0.93 (95% CL)	$-0.78^{+0.39}_{-0.31}$
$G_{\rm N}/G$ (z=0)	> 0.9981 (95% CL)	> 0.9985 (95% CL)	$0.9987^{+0.00064}_{-0.00051}$
$\Omega_{\rm m}$	$0.306^{+0.015}_{-0.018}$	0.3029 ± 0.0076	0.2905 ± 0.0068
σ_8	$0.815^{+0.025}_{-0.014}$	$0.821^{+0.014}_{-0.010}$	0.832 ± 0.013
r_s [Mpc]	$146.18^{+0.78}_{-0.38}$	$146.31^{+0.71}_{-0.37}$	$145.56^{+0.78}_{-0.69}$
$\Delta\chi^2$	3.0	0.2	-3.3

Table 5. Constraints on main and derived parameters (at 68% CL if not otherwise stated) considering P18 in combination with BAO and BAO + R19 for the IG+m_ν model.

	P18	P18 + BAO	P18 + BAO + R19
$\omega_{\rm b}$	0.02240 ± 0.00016	0.02242 ± 0.00013	0.02252 ± 0.00013
$\omega_{\rm c}$	0.1203 ± 0.0013	0.12011 ± 0.00097	0.1197 ± 0.0010
H_0 [km s^{-1}Mpc^{-1}]	68.0 ± 1.4 (3.0σ)	$68.31^{+0.62}_{-0.69}$ (3.7σ)	$69.62\ 0.71$ (2.8σ)
τ	$0.0563^{+0.0063}_{-0.0080}$	$0.0564^{+0.0065}_{-0.0077}$	$0.0576^{+0.0067}_{-0.0077}$
$\ln\left(10^{10}A_{\rm s}\right)$	$3.051^{+0.013}_{-0.016}$	$3.047^{+0.013}_{-0.015}$	$3.054^{+0.013}_{-0.016}$
$n_{\rm s}$	0.9674 ± 0.0053	0.9681 ± 0.0043	0.9720 ± 0.0041
$N_{\rm pl}$ [M$_{\rm pl}$]	< 1.000026 (95% CL)	< 1.000024 (95% CL)	$1.000019^{+0.000017}_{-0.000018}$ (95% CL)
m_ν [eV]	< 0.28 (95% CL)	< 0.16 (95% CL)	< 0.13 (95% CL)
γ_{PN}	> 0.999926 (95% CL)	> 0.999924 (95% CL)	$0.9999192^{+0.000009}_{-0.000011}$ (95% CL)
β_{PN}	< 1.0000021 (95% CL)	< 1.0000020 (95% CL)	< 1.0000030 (95% CL)
$\delta G_{\rm N}/G_{\rm N}$	> -0.024 (95% CL)	> -0.023 (95% CL)	$-0.0181^{+0.0099}_{-0.0082}$
$10^{13}\dot{G}_{\rm N}/G_{\rm N}$ (z=0) [yr^{-1}]	$> -3.6 \times 10^{-9}$ (95% CL)	$> -3.3 \times 10^{-9}$ (95% CL)	$(-2.7^{+1.5}_{-1.2}) \times 10^{-9}$
$G_{\rm N}/G$ (z=0)	> 0.999987 (95% CL)	> 0.9999988 (95% CL)	$0.9999904^{+0.0000054}_{-0.0000043}$
$\Omega_{\rm m}$	$0.309^{+0.011}_{-0.015}$	0.3047 ± 0.0067	0.2935 ± 0.0064
σ_8	0.814 ± 0.010	$0.820^{+0.013}_{-0.010}$	0.831 ± 0.012
r_s [Mpc]	$146.52^{+0.47}_{-0.34}$	$146.58^{+0.47}_{-0.31}$	$146.26^{+0.55}_{-0.48}$
$\Delta\chi^2$	3.0	0.0	-1.5

Table 6. Constraints on main and derived parameters (at 68% CL if not otherwise stated) considering P18 in combination with BAO and BAO + R19 for the CC+m_ν model.

A.4 Degeneracy with the neutrino sector: $(N_{\mathrm{eff}},\ m_\nu)$

	P18	P18 + BAO	P18 + BAO + R19
ω_{b}	0.02218 ± 0.00022	$0.02220^{+0.00022}_{-0.00019}$	0.02250 ± 0.00020
ω_{c}	0.1162 ± 0.0034	0.1164 ± 0.0031	0.1208 ± 0.0030
H_0 [km s^{-1}Mpc^{-1}]	$67.7^{+2.0}_{-2.4}$ (2.6σ)	$67.6 \pm 1.2 (3.5\sigma)$	70.25 ± 0.92 (2.2σ)
τ	$0.0556^{+0.0065}_{-0.0083}$	$0.0554^{+0.0065}_{-0.0073}$	$0.0576^{+0.0063}_{-0.0081}$
$\ln\left(10^{10}A_{\mathrm{s}}\right)$	$3.039^{-0.018}_{+0.016}$	3.039 ± 0.016	3.056 ± 0.016
n_{s}	0.9577 ± 0.0086	0.9582 ± 0.0076	0.9710 ± 0.0071
ζ_{IG}	< 0.0070 (95% CL)	< 0.0047 (95% CL)	< 0.0053 (95% CL)
m_ν [eV]	< 0.26 (95% CL)	< 0.19 (95% CL)	< 0.19 (95% CL)
N_{eff}	2.74 ± 0.22	2.77 ± 0.20	3.08 ± 0.20
ξ	< 0.0018 (95% CL)	< 0.0012 (95% CL)	< 0.0013 (95% CL)
γ_{PN}	> 0.9931 (95% CL)	> 0.9954 (95% CL)	> 0.9948 (95% CL)
$\delta G_{\mathrm{N}}/G_{\mathrm{N}}$ (z=0)	> -0.050 (95% CL)	> -0.034 (95% CL)	> -0.038 (95% CL)
$10^{13}\dot{G}_{\mathrm{N}}/G_{\mathrm{N}}$ (z=0) [yr^{-1}]	> -2.0 (95% CL)	> -1.4 (95% CL)	> 1.6 (95% CL)
G_{N}/G (z=0)	> 0.9966 (95% CL)	> 0.9977 (95% CL)	> 0.9974 (95% CL)
Ω_{m}	$0.303^{+0.022}_{-0.019}$	0.3035 ± 0.0081	0.2904 ± 0.0069
σ_8	$0.814^{+0.025}_{-0.019}$	$0.815^{+0.015}_{-0.012}$	$0.833^{+0.013}_{-0.011}$
r_s [Mpc]	148.6 ± 1.9	148.6 ± 1.8	145.3 ± 1.6
$\Delta\chi^2$	1.1	0.5	-2.5

Table 7. Constraints on main and derived parameters (at 68% CL if not otherwise stated) considering P18 in combination with BAO and BAO + R19 for the IG+N_{eff}+m_ν model.

	P18	P18 + BAO	P18 + BAO + R19
ω_{b}	0.02217 ± 0.00022	0.02222 ± 0.00020	0.02257 ± 0.00018
ω_{c}	0.1158 ± 0.0034	0.1158 ± 0.0032	0.1212 ± 0.0031
H_0 [km s^{-1}Mpc^{-1}]	66.7 ± 1.8 (3.2σ)	$67.2 \pm 1.1 (3.8\sigma)$	69.96 ± 0.93 (2.1σ)
τ	$0.0554^{+0.0064}_{-0.0076}$	$0.0556^{+0.0063}_{-0.0075}$	$0.0577^{+0.0069}_{-0.0082}$
$\ln\left(10^{10}A_{\mathrm{s}}\right)$	3.039 ± 0.017	3.039 ± 0.016	3.057 ± 0.016
n_{s}	0.9582 ± 0.0084	0.9596 ± 0.0074	0.9745 ± 0.0064
N_{pl} [M$_{\mathrm{pl}}$]	< 1.000050 (95% CL)	< 1.000042 (95% CL)	< 1.000040 (95% CL)
m_ν [eV]	< 0.26 (95% CL)	< 0.17 (95% CL)	< 0.14 (95% CL)
N_{eff}	2.73 ± 0.21	2.75 ± 0.21	3.14 ± 0.20
γ_{PN}	> 0.999950 (95% CL)	> 0.9958 (95% CL)	> 0.9960 (95% CL)
β_{PN}	< 1.0000041 (95% CL)	< 1.0000035 (95% CL)	< 1.0000033 (95% CL)
$\delta G_{\mathrm{N}}/G_{\mathrm{N}}$ (z=0)	> -0.046 (95% CL)	> -0.040 (95% CL)	> -0.037 (95% CL)
$10^{13}\dot{G}_{\mathrm{N}}/G_{\mathrm{N}}$ (z=0) [yr^{-1}]	$> -6.7 \times 10^{-9}$ (95% CL)	$> -5.7 \times 10^{-9}$ (95% CL)	$> -5.5 \times 10^{-9}$ (95% CL)
G_{N}/G (z=0)	> 0.999975 (95% CL)	> 0.999979 (95% CL)	> 0.999980 (95% CL)
Ω_{m}	$0.310^{+0.016}_{-0.018}$	0.3056 ± 0.0074	0.2939 ± 0.0064
σ_8	$0.808^{+0.024}_{-0.015}$	$0.814^{+0.015}_{-0.011}$	0.833 ± 0.012
r_s [Mpc]	$149.3^{+1.8}_{-2.1}$	149.2 ± 1.9	145.4 ± 1.7
$\Delta\chi^2$	3.0	0.4	-0.6

Table 8. Constraints on main and derived parameters (at 68% CL if not otherwise stated) considering P18 in combination with BAO and BAO + R19 for the CC+N_{eff}+m_ν model.

References

[1] A.G. Riess et al., *A 2.4% determination of the local value of the Hubble constant*, Astrophys. J. **826** (2016) 56 [arXiv:1604.01424] [inSPIRE].

[2] A.G. Riess et al., *Milky Way Cepheid standards for measuring cosmic distances and application to Gaia DR2: implications for the Hubble constant*, Astrophys. J. **861** (2018) 126 [arXiv:1804.10655] [inSPIRE].

[3] V. Bonvin et al., *H0LiCOW — V. New COSMOGRAIL time delays of HE 0435-1223: H_0 to 3.8 per cent precision from strong lensing in a flat ΛCDM model*, Mon. Not. Roy. Astron. Soc. **465** (2017) 4914 [arXiv:1607.01790] [inSPIRE].

[4] S. Birrer et al., *H0LiCOW — IX. Cosmographic analysis of the doubly imaged quasar SDSS 1206+4332 and a new measurement of the Hubble constant*, Mon. Not. Roy. Astron. Soc. **484** (2019) 4726 [arXiv:1809.01274] [inSPIRE].

[5] K.C. Wong et al., *H0LiCOW — XIII. A 2.4% measurement of H_0 from lensed quasars: 5.3σ tension between early and late-Universe probes*, arXiv:1907.04869 [inSPIRE].

[6] PLANCK collaboration, *Planck 2015 results. XIII. Cosmological parameters*, Astron. Astrophys. **594** (2016) A13 [arXiv:1502.01589] [inSPIRE].

[7] PLANCK collaboration, *Planck 2018 results. VI. Cosmological parameters*, Astron. Astrophys. **641** (2020) A6 [arXiv:1807.06209] [inSPIRE].

[8] A.G. Riess, S. Casertano, W. Yuan, L.M. Macri and D. Scolnic, *Large Magellanic Cloud Cepheid standards provide a 1% foundation for the determination of the Hubble constant and stronger evidence for physics beyond ΛCDM*, Astrophys. J. **876** (2019) 85 [arXiv:1903.07603] [inSPIRE].

[9] A.G. Riess et al., *New parallaxes of galactic Cepheids from spatially scanning the Hubble Space Telescope: implications for the Hubble constant*, Astrophys. J. **855** (2018) 136 [arXiv:1801.01120] [inSPIRE].

[10] G.E. Addison et al., *Quantifying discordance in the 2015 Planck CMB spectrum*, Astrophys. J. **818** (2016) 132 [arXiv:1511.00055] [inSPIRE].

[11] PLANCK collaboration, *Planck intermediate results. LI. Features in the cosmic microwave background temperature power spectrum and shifts in cosmological parameters*, Astron. Astrophys. **607** (2017) A95 [arXiv:1608.02487] [inSPIRE].

[12] K. Aylor, M. Joy, L. Knox, M. Millea, S. Raghunathan and W.L.K. Wu, *Sounds discordant: classical distance ladder & ΛCDM-based Determinations of the cosmological sound horizon*, Astrophys. J. **874** (2019) 4 [arXiv:1811.00537] [inSPIRE].

[13] G. Efstathiou, *H0 revisited*, Mon. Not. Roy. Astron. Soc. **440** (2014) 1138 [arXiv:1311.3461] [inSPIRE].

[14] M. Rigault et al., *Confirmation of a star formation bias in Type Ia supernova distances and its effect on measurement of the Hubble constant*, Astrophys. J. **802** (2015) 20 [arXiv:1412.6501] [inSPIRE].

[15] NEARBY SUPERNOVA FACTORY collaboration, *Strong dependence of Type Ia supernova standardization on the local specific star formation rate*, arXiv:1806.03849 [inSPIRE].

[16] W.L. Freedman et al., *The Carnegie-Chicago Hubble program. VIII. An independent determination of the Hubble constant based on the tip of the Red Giant Branch*, arXiv:1907.05922 [inSPIRE].

[17] D.O. Jones et al., *Should Type Ia supernova distances be corrected for their local environments?*, Astrophys. J. **867** (2018) 108 [arXiv:1805.05911] [inSPIRE].

[18] B.M. Rose, P.M. Garnavich and M.A. Berg, *Think global, act local: the influence of environment age and host mass on Type Ia supernova light curves*, *Astrophys. J.* **874** (2019) 32 [arXiv:1902.01433] [inSPIRE].

[19] W. Yuan, A.G. Riess, L.M. Macri, S. Casertano and D. Scolnic, *Consistent calibration of the tip of the red giant branch in the Large Magellanic Cloud on the Hubble Space Telescope photometric system and a re-determination of the Hubble constant*, *Astrophys. J.* **886** (2019) 61 [arXiv:1908.00993] [inSPIRE].

[20] S. Dhawan, D. Brout, D. Scolnic, A. Goobar, A.G. Riess and V. Miranda, *Cosmological model insensitivity of local H_0 from the Cepheid distance ladder*, *Astrophys. J.* **894** (2020) 54 [arXiv:2001.09260] [inSPIRE].

[21] W.L. Freedman et al., *Calibration of the Tip of the Red Giant Branch (TRGB)*, arXiv:2002.01550 [inSPIRE].

[22] E. Mörtsell and S. Dhawan, *Does the Hubble constant tension call for new physics?*, *JCAP* **09** (2018) 025 [arXiv:1801.07260] [inSPIRE].

[23] L. Knox and M. Millea, *Hubble constant hunter's guide*, *Phys. Rev. D* **101** (2020) 043533 [arXiv:1908.03663] [inSPIRE].

[24] E. Di Valentino, A. Melchiorri and J. Silk, *Reconciling Planck with the local value of H_0 in extended parameter space*, *Phys. Lett. B* **761** (2016) 242 [arXiv:1606.00634] [inSPIRE].

[25] E. Di Valentino, A. Melchiorri, E.V. Linder and J. Silk, *Constraining dark energy dynamics in extended parameter space*, *Phys. Rev. D* **96** (2017) 023523 [arXiv:1704.00762] [inSPIRE].

[26] S. Vagnozzi, *New physics in light of the H_0 tension: an alternative view*, *Phys. Rev. D* **102** (2020) 023518 [arXiv:1907.07569] [inSPIRE].

[27] E. Di Valentino, E.V. Linder and A. Melchiorri, *Vacuum phase transition solves the H_0 tension*, *Phys. Rev. D* **97** (2018) 043528 [arXiv:1710.02153] [inSPIRE].

[28] N. Khosravi, S. Baghram, N. Afshordi and N. Altamirano, *H_0 tension as a hint for a transition in gravitational theory*, *Phys. Rev. D* **99** (2019) 103526 [arXiv:1710.09366] [inSPIRE].

[29] A. Banihashemi, N. Khosravi and A.H. Shirazi, *Ginzburg-Landau theory of dark energy: a framework to study both temporal and spatial cosmological tensions simultaneously*, *Phys. Rev. D* **99** (2019) 083509 [arXiv:1810.11007] [inSPIRE].

[30] A. Banihashemi, N. Khosravi and A.H. Shirazi, *Phase transition in the dark sector as a proposal to lessen cosmological tensions*, *Phys. Rev. D* **101** (2020) 123521 [arXiv:1808.02472] [inSPIRE].

[31] G. Benevento, W. Hu and M. Raveri, *Can late dark energy transitions raise the Hubble constant?*, *Phys. Rev. D* **101** (2020) 103517 [arXiv:2002.11707] [inSPIRE].

[32] S. Kumar and R.C. Nunes, *Probing the interaction between dark matter and dark energy in the presence of massive neutrinos*, *Phys. Rev. D* **94** (2016) 123511 [arXiv:1608.02454] [inSPIRE].

[33] E. Di Valentino, A. Melchiorri and O. Mena, *Can interacting dark energy solve the H_0 tension?*, *Phys. Rev. D* **96** (2017) 043503 [arXiv:1704.08342] [inSPIRE].

[34] W. Yang, S. Pan, E. Di Valentino, R.C. Nunes, S. Vagnozzi and D.F. Mota, *Tale of stable interacting dark energy, observational signatures, and the H_0 tension*, *JCAP* **09** (2018) 019 [arXiv:1805.08252] [inSPIRE].

[35] E. Di Valentino, A. Melchiorri, O. Mena and S. Vagnozzi, *Nonminimal dark sector physics and cosmological tensions*, *Phys. Rev. D* **101** (2020) 063502 [arXiv:1910.09853] [inSPIRE].

[36] A. Gómez-Valent, V. Pettorino and L. Amendola, *Update on coupled dark energy and the H_0 tension*, *Phys. Rev. D* **101** (2020) 123513 [arXiv:2004.00610] [inSPIRE].

[37] H. Miao and Z. Huang, *The H_0 tension in non-flat QCDM cosmology*, *Astrophys. J.* **868** (2018) 20 [`arXiv:1803.07320`] [ɪɴSPIRE].

[38] G.E. Addison, D.J. Watts, C.L. Bennett, M. Halpern, G. Hinshaw and J.L. Weiland, *Elucidating ΛCDM: impact of baryon acoustic oscillation measurements on the Hubble constant discrepancy*, *Astrophys. J.* **853** (2018) 119 [`arXiv:1707.06547`] [ɪɴSPIRE].

[39] F. Beutler et al., *The 6dF galaxy survey: baryon acoustic oscillations and the local Hubble constant*, *Mon. Not. Roy. Astron. Soc.* **416** (2011) 3017 [`arXiv:1106.3366`] [ɪɴSPIRE].

[40] A.J. Ross, L. Samushia, C. Howlett, W.J. Percival, A. Burden and M. Manera, *The clustering of the SDSS DR7 main Galaxy sample — I. A 4 per cent distance measure at $z = 0.15$*, *Mon. Not. Roy. Astron. Soc.* **449** (2015) 835 [`arXiv:1409.3242`] [ɪɴSPIRE].

[41] BOSS collaboration, *The clustering of galaxies in the completed SDSS-III Baryon Oscillation Spectroscopic Survey: cosmological analysis of the DR12 galaxy sample*, *Mon. Not. Roy. Astron. Soc.* **470** (2017) 2617 [`arXiv:1607.03155`] [ɪɴSPIRE].

[42] PLANCK collaboration, *Planck 2018 results. I. Overview and the cosmological legacy of Planck*, *Astron. Astrophys.* **641** (2020) A1 [`arXiv:1807.06205`] [ɪɴSPIRE].

[43] J.L. Bernal, L. Verde and A.G. Riess, *The trouble with H_0*, *JCAP* **10** (2016) 019 [`arXiv:1607.05617`] [ɪɴSPIRE].

[44] F.-Y. Cyr-Racine and K. Sigurdson, *Limits on neutrino-neutrino scattering in the early universe*, *Phys. Rev. D* **90** (2014) 123533 [`arXiv:1306.1536`] [ɪɴSPIRE].

[45] L. Lancaster, F.-Y. Cyr-Racine, L. Knox and Z. Pan, *A tale of two modes: Neutrino free-streaming in the early universe*, *JCAP* **07** (2017) 033 [`arXiv:1704.06657`] [ɪɴSPIRE].

[46] M.A. Buen-Abad, M. Schmaltz, J. Lesgourgues and T. Brinckmann, *Interacting dark sector and precision cosmology*, *JCAP* **01** (2018) 008 [`arXiv:1708.09406`] [ɪɴSPIRE].

[47] E. Di Valentino, C. Bøehm, E. Hivon and F.R. Bouchet, *Reducing the H_0 and σ_8 tensions with dark matter-neutrino interactions*, *Phys. Rev. D* **97** (2018) 043513 [`arXiv:1710.02559`] [ɪɴSPIRE].

[48] F. D'Eramo, R.Z. Ferreira, A. Notari and J.L. Bernal, *Hot axions and the H_0 tension*, *JCAP* **11** (2018) 014 [`arXiv:1808.07430`] [ɪɴSPIRE].

[49] V. Poulin, K.K. Boddy, S. Bird and M. Kamionkowski, *Implications of an extended dark energy cosmology with massive neutrinos for cosmological tensions*, *Phys. Rev. D* **97** (2018) 123504 [`arXiv:1803.02474`] [ɪɴSPIRE].

[50] C.D. Kreisch, F.-Y. Cyr-Racine and O. Doré, *Neutrino puzzle: anomalies, interactions, and cosmological tensions*, *Phys. Rev. D* **101** (2020) 123505 [`arXiv:1902.00534`] [ɪɴSPIRE].

[51] N. Blinov, K.J. Kelly, G.Z. Krnjaic and S.D. McDermott, *Constraining the self-interacting neutrino interpretation of the Hubble tension*, *Phys. Rev. Lett.* **123** (2019) 191102 [`arXiv:1905.02727`] [ɪɴSPIRE].

[52] V. Poulin, T.L. Smith, T. Karwal and M. Kamionkowski, *Early dark energy can resolve the Hubble tension*, *Phys. Rev. Lett.* **122** (2019) 221301 [`arXiv:1811.04083`] [ɪɴSPIRE].

[53] P. Agrawal, F.-Y. Cyr-Racine, D. Pinner and L. Randall, *Rock'n'roll solutions to the Hubble tension*, `arXiv:1904.01016` [ɪɴSPIRE].

[54] T.L. Smith, V. Poulin and M.A. Amin, *Oscillating scalar fields and the Hubble tension: a resolution with novel signatures*, *Phys. Rev. D* **101** (2020) 063523 [`arXiv:1908.06995`] [ɪɴSPIRE].

[55] S. Alexander and E. McDonough, *Axion-dilaton destabilization and the Hubble tension*, *Phys. Lett. B* **797** (2019) 134830 [`arXiv:1904.08912`] [ɪɴSPIRE].

[56] M.-X. Lin, G. Benevento, W. Hu and M. Raveri, *Acoustic dark energy: potential conversion of the Hubble tension*, *Phys. Rev. D* **100** (2019) 063542 [arXiv:1905.12618] [INSPIRE].

[57] M. Braglia, W.T. Emond, F. Finelli, A.E. Gumrukcuoglu and K. Koyama, *Unified framework for early dark energy from α-attractors*, *Phys. Rev. D* **102** (2020) 083513 [arXiv:2005.14053] [INSPIRE].

[58] D.K. Hazra, A. Shafieloo and T. Souradeep, *Parameter discordance in Planck CMB and low-redshift measurements: projection in the primordial power spectrum*, *JCAP* **04** (2019) 036 [arXiv:1810.08101] [INSPIRE].

[59] M. Liu and Z. Huang, *Band-limited features in the primordial power spectrum do not resolve the Hubble tension*, *Astrophys. J.* **897** (2020) 166 [arXiv:1910.05670] [INSPIRE].

[60] C.-T. Chiang and A. Slosar, *Inferences of H_0 in presence of a non-standard recombination*, arXiv:1811.03624 [INSPIRE].

[61] M. Liu, Z. Huang, X. Luo, H. Miao, N.K. Singh and L. Huang, *Can non-standard recombination resolve the Hubble tension?*, *Sci. China Phys. Mech. Astron.* **63** (2020) 290405 [arXiv:1912.00190] [INSPIRE].

[62] C. Umiltà, M. Ballardini, F. Finelli and D. Paoletti, *CMB and BAO constraints for an induced gravity dark energy model with a quartic potential*, *JCAP* **08** (2015) 017 [arXiv:1507.00718] [INSPIRE].

[63] M. Ballardini, F. Finelli, C. Umiltà and D. Paoletti, *Cosmological constraints on induced gravity dark energy models*, *JCAP* **05** (2016) 067 [arXiv:1601.03387] [INSPIRE].

[64] R.C. Nunes, *Structure formation in $f(T)$ gravity and a solution for H_0 tension*, *JCAP* **05** (2018) 052 [arXiv:1802.02281] [INSPIRE].

[65] M.-X. Lin, M. Raveri and W. Hu, *Phenomenology of modified gravity at recombination*, *Phys. Rev. D* **99** (2019) 043514 [arXiv:1810.02333] [INSPIRE].

[66] M. Rossi et al., *Cosmological constraints on post-Newtonian parameters in effectively massless scalar-tensor theories of gravity*, *Phys. Rev. D* **100** (2019) 103524 [arXiv:1906.10218] [INSPIRE].

[67] J. Solà Peracaula, A. Gomez-Valent, J. de Cruz Pérez and C. Moreno-Pulido, *Brans-Dicke gravity with a cosmological constant smoothes out ΛCDM tensions*, *Astrophys. J. Lett.* **886** (2019) L6 [arXiv:1909.02554] [INSPIRE].

[68] M. Zumalacarregui, *Gravity in the era of equality: towards solutions to the Hubble problem without fine-tuned initial conditions*, *Phys. Rev. D* **102** (2020) 023523 [arXiv:2003.06396] [INSPIRE].

[69] D. Wang and D. Mota, *Can $f(T)$ gravity resolve the H_0 tension?*, *Phys. Rev. D* **102** (2020) 063530 [arXiv:2003.10095] [INSPIRE].

[70] G. Ballesteros, A. Notari and F. Rompineve, *The H_0 tension: ΔG_N vs. ΔN_{eff}*, arXiv:2004.05049 [INSPIRE].

[71] M. Braglia et al., *Larger value for H_0 by an evolving gravitational constant*, *Phys. Rev. D* **102** (2020) 023529 [arXiv:2004.11161] [INSPIRE].

[72] H. Motohashi, A.A. Starobinsky and J. Yokoyama, *Cosmology Based on $f(R)$ gravity admits 1 eV sterile neutrinos*, *Phys. Rev. Lett.* **110** (2013) 121302 [arXiv:1203.6828] [INSPIRE].

[73] A.S. Chudaykin, D.S. Gorbunov, A.A. Starobinsky and R.A. Burenin, *Cosmology based on $f(R)$ gravity with Script $O(1)$ eV sterile neutrino*, *JCAP* **05** (2015) 004 [arXiv:1412.5239] [INSPIRE].

[74] S. Vagnozzi et al., *Unveiling ν secrets with cosmological data: neutrino masses and mass hierarchy*, *Phys. Rev. D* **96** (2017) 123503 [arXiv:1701.08172] [INSPIRE].

[75] S. Roy Choudhury and S. Hannestad, *Updated results on neutrino mass and mass hierarchy from cosmology with Planck 2018 likelihoods*, *JCAP* **07** (2020) 037 [arXiv:1907.12598] [INSPIRE].

[76] A. Barreira, B. Li, C. Baugh and S. Pascoli, *Modified gravity with massive neutrinos as a testable alternative cosmological model*, *Phys. Rev. D* **90** (2014) 023528 [arXiv:1404.1365] [INSPIRE].

[77] PARTICLE DATA GROUP collaboration, *Review of particle physics*, *Phys. Rev. D* **98** (2018) 030001 [INSPIRE].

[78] SIMONS OBSERVATORY collaboration, *The Simons observatory: science goals and forecasts*, *JCAP* **02** (2019) 056 [arXiv:1808.07445] [INSPIRE].

[79] CMB-S4 collaboration, *CMB-S4 science book, first edition*, arXiv:1610.02743 [INSPIRE].

[80] DESI collaboration, *The DESI experiment, a whitepaper for Snowmass 2013*, arXiv:1308.0847 [INSPIRE].

[81] EUCLID collaboration, *Euclid definition study report*, arXiv:1110.3193 [INSPIRE].

[82] EUCLID THEORY WORKING GROUP collaboration, *Cosmology and fundamental physics with the Euclid satellite*, *Living Rev. Rel.* **16** (2013) 6 [arXiv:1206.1225] [INSPIRE].

[83] LSST SCIENCE, LSST PROJECT collaboration, *LSST science book, version 2.0*, arXiv:0912.0201 [INSPIRE].

[84] SKA COSMOLOGY SWG collaboration, *Overview of Cosmology with the SKA*, PoS(AASKA14)016 [arXiv:1501.04076] [INSPIRE].

[85] SKA collaboration, *Cosmology with Phase 1 of the Square Kilometre Array: red book 2018: technical specifications and performance forecasts*, *Publ. Astron. Soc. Austral.* **37** (2020) e007 [arXiv:1811.02743] [INSPIRE].

[86] T. Brinckmann, D.C. Hooper, M. Archidiacono, J. Lesgourgues and T. Sprenger, *The promising future of a robust cosmological neutrino mass measurement*, *JCAP* **01** (2019) 059 [arXiv:1808.05955] [INSPIRE].

[87] D. Alonso, E. Bellini, P.G. Ferreira and M. Zumalacárregui, *Observational future of cosmological scalar-tensor theories*, *Phys. Rev. D* **95** (2017) 063502 [arXiv:1610.09290] [INSPIRE].

[88] M. Ballardini, D. Sapone, C. Umiltà, F. Finelli and D. Paoletti, *Testing extended Jordan-Brans-Dicke theories with future cosmological observations*, *JCAP* **05** (2019) 049 [arXiv:1902.01407] [INSPIRE].

[89] N. Bellomo, E. Bellini, B. Hu, R. Jimenez, C. Pena-Garay and L. Verde, *Hiding neutrino mass in modified gravity cosmologies*, *JCAP* **02** (2017) 043 [arXiv:1612.02598] [INSPIRE].

[90] P. Jordan, *Formation of the stars and development of the universe*, *Nature* **164** (1949) 637 [INSPIRE].

[91] C. Brans and R.H. Dicke, *Mach's principle and a relativistic theory of gravitation*, *Phys. Rev.* **124** (1961) 925 [INSPIRE].

[92] X.-l. Chen and M. Kamionkowski, *Cosmic microwave background temperature and polarization anisotropy in Brans-Dicke cosmology*, *Phys. Rev. D* **60** (1999) 104036 [astro-ph/9905368] [INSPIRE].

[93] R. Nagata, T. Chiba and N. Sugiyama, *WMAP constraints on scalar-tensor cosmology and the variation of the gravitational constant*, *Phys. Rev. D* **69** (2004) 083512 [astro-ph/0311274] [INSPIRE].

[94] V. Acquaviva, C. Baccigalupi, S.M. Leach, A.R. Liddle and F. Perrotta, *Structure formation constraints on the Jordan-Brans-Dicke theory*, *Phys. Rev. D* **71** (2005) 104025 [astro-ph/0412052] [INSPIRE].

[95] A. Avilez and C. Skordis, *Cosmological constraints on Brans-Dicke theory*, *Phys. Rev. Lett.* **113** (2014) 011101 [arXiv:1303.4330] [INSPIRE].

[96] Y.-C. Li, F.-Q. Wu and X. Chen, *Constraints on the Brans-Dicke gravity theory with the Planck data*, *Phys. Rev. D* **88** (2013) 084053 [arXiv:1305.0055] [INSPIRE].

[97] J. Ooba, K. Ichiki, T. Chiba and N. Sugiyama, *Planck constraints on scalar-tensor cosmology and the variation of the gravitational constant*, *Phys. Rev. D* **93** (2016) 122002 [arXiv:1602.00809] [INSPIRE].

[98] G.W. Horndeski, *Second-order scalar-tensor field equations in a four-dimensional space*, *Int. J. Theor. Phys.* **10** (1974) 363 [INSPIRE].

[99] J.-P. Uzan, *Cosmological scaling solutions of nonminimally coupled scalar fields*, *Phys. Rev. D* **59** (1999) 123510 [gr-qc/9903004] [INSPIRE].

[100] F. Perrotta, C. Baccigalupi and S. Matarrese, *Extended quintessence*, *Phys. Rev. D* **61** (1999) 023507 [astro-ph/9906066] [INSPIRE].

[101] N. Bartolo and M. Pietroni, *Scalar tensor gravity and quintessence*, *Phys. Rev. D* **61** (2000) 023518 [hep-ph/9908521] [INSPIRE].

[102] L. Amendola, *Scaling solutions in general nonminimal coupling theories*, *Phys. Rev. D* **60** (1999) 043501 [astro-ph/9904120] [INSPIRE].

[103] T. Chiba, *Quintessence, the gravitational constant, and gravity*, *Phys. Rev. D* **60** (1999) 083508 [gr-qc/9903094] [INSPIRE].

[104] B. Boisseau, G. Esposito-Farese, D. Polarski and A.A. Starobinsky, *Reconstruction of a scalar tensor theory of gravity in an accelerating universe*, *Phys. Rev. Lett.* **85** (2000) 2236 [gr-qc/0001066] [INSPIRE].

[105] C.M. Will, *The confrontation between general relativity and experiment*, *Living Rev. Rel.* **17** (2014) 4 [arXiv:1403.7377] [INSPIRE].

[106] B. Bertotti, L. Iess and P. Tortora, *A test of general relativity using radio links with the Cassini spacecraft*, *Nature* **425** (2003) 374 [INSPIRE].

[107] A.Y. Kamenshchik, E.O. Pozdeeva, A.A. Starobinsky, A. Tronconi, G. Venturi and S.Y. Vernov, *Induced gravity, and minimally and conformally coupled scalar fields in Bianchi-I cosmological models*, *Phys. Rev. D* **97** (2018) 023536 [arXiv:1710.02681] [INSPIRE].

[108] B. Audren, J. Lesgourgues, K. Benabed and S. Prunet, *Conservative constraints on early cosmology: an illustration of the Monte Python cosmological parameter inference code*, *JCAP* **02** (2013) 001 [arXiv:1210.7183] [INSPIRE].

[109] T. Brinckmann and J. Lesgourgues, *MontePython 3: boosted MCMC sampler and other features*, *Phys. Dark Univ.* **24** (2019) 100260 [arXiv:1804.07261] [INSPIRE].

[110] J. Lesgourgues, *The Cosmic Linear Anisotropy Solving System (CLASS) I: overview*, arXiv:1104.2932 [INSPIRE].

[111] D. Blas, J. Lesgourgues and T. Tram, *The Cosmic Linear Anisotropy Solving System (CLASS) II: approximation schemes*, *JCAP* **07** (2011) 034 [arXiv:1104.2933] [INSPIRE].

[112] A. Lewis, *GetDist: a Python package for analysing Monte Carlo samples*, arXiv:1910.13970 [INSPIRE].

[113] D. Paoletti, M. Braglia, F. Finelli, M. Ballardini and C. Umiltà, *Isocurvature fluctuations in the effective Newton's constant*, *Phys. Dark Univ.* **25** (2019) 100307 [arXiv:1809.03201].

[114] PLANCK collaboration, *Planck 2018 results. V. CMB power spectra and likelihoods*, *Astron. Astrophys.* **641** (2020) A5 [arXiv:1907.12875] [INSPIRE].

[115] PLANCK collaboration, *Planck 2018 results. VIII. Gravitational lensing*, *Astron. Astrophys.* **641** (2020) A8 [arXiv:1807.06210] [INSPIRE].

[116] BOSS collaboration, *The clustering of galaxies in the completed SDSS-III Baryon Oscillation Spectroscopic Survey: observational systematics and baryon acoustic oscillations in the correlation function*, *Mon. Not. Roy. Astron. Soc.* **464** (2017) 1168 [arXiv:1607.03145] [INSPIRE].

[117] M. Vargas-Magaña et al., *The clustering of galaxies in the completed SDSS-III Baryon Oscillation Spectroscopic Survey: theoretical systematics and Baryon Acoustic Oscillations in the galaxy correlation function*, *Mon. Not. Roy. Astron. Soc.* **477** (2018) 1153 [arXiv:1610.03506] [INSPIRE].

[118] BOSS collaboration, *The clustering of galaxies in the completed SDSS-III Baryon Oscillation Spectroscopic Survey: baryon acoustic oscillations in the Fourier space*, *Mon. Not. Roy. Astron. Soc.* **464** (2017) 3409 [arXiv:1607.03149] [INSPIRE].

[119] PLANCK collaboration, *Planck 2015 results. I. Overview of products and scientific results*, *Astron. Astrophys.* **594** (2016) A1 [arXiv:1502.01582] [INSPIRE].

[120] PLANCK collaboration, *Planck 2015 results. XI. CMB power spectra, likelihoods, and robustness of parameters*, *Astron. Astrophys.* **594** (2016) A11 [arXiv:1507.02704] [INSPIRE].

[121] J.G. Williams, S.G. Turyshev and D.H. Boggs, *Progress in lunar laser ranging tests of relativistic gravity*, *Phys. Rev. Lett.* **93** (2004) 261101 [gr-qc/0411113] [INSPIRE].

[122] BOSS collaboration, *The clustering of galaxies in the SDSS-III Baryon Oscillation Spectroscopic Survey: baryon acoustic oscillations in the Data Releases 10 and 11 Galaxy samples*, *Mon. Not. Roy. Astron. Soc.* **441** (2014) 24 [arXiv:1312.4877] [INSPIRE].

[123] S. Hannestad, *Primordial neutrinos*, *Ann. Rev. Nucl. Part. Sci.* **56** (2006) 137 [hep-ph/0602058] [INSPIRE].

[124] J. Lesgourgues, G. Mangano, G. Miele and S. Pastor, *Neutrino cosmology*, Cambridge UNiversity Press, Cambridge U.K. (2013).

[125] S. Dodelson and M.S. Turner, *Nonequilibrium neutrino statistical mechanics in the expanding universe*, *Phys. Rev. D* **46** (1992) 3372 [INSPIRE].

[126] B.D. Fields, S. Dodelson and M.S. Turner, *Effect of neutrino heating on primordial nucleosynthesis*, *Phys. Rev. D* **47** (1993) 4309 [astro-ph/9210007] [INSPIRE].

[127] A.D. Dolgov and M. Fukugita, *Nonequilibrium effect of the neutrino distribution on primordial helium synthesis*, *Phys. Rev. D* **46** (1992) 5378 [INSPIRE].

[128] G. Mangano, G. Miele, S. Pastor, T. Pinto, O. Pisanti and P.D. Serpico, *Relic neutrino decoupling including flavor oscillations*, *Nucl. Phys. B* **729** (2005) 221 [hep-ph/0506164] [INSPIRE].

[129] S. Bashinsky and U. Seljak, *Neutrino perturbations in CMB anisotropy and matter clustering*, *Phys. Rev. D* **69** (2004) 083002 [astro-ph/0310198] [INSPIRE].

[130] S. Hannestad, *Neutrino masses and the dark energy equation of state — Relaxing the cosmological neutrino mass bound*, *Phys. Rev. Lett.* **95** (2005) 221301 [astro-ph/0505551] [INSPIRE].

[131] J. Lesgourgues and S. Pastor, *Massive neutrinos and cosmology*, *Phys. Rept.* **429** (2006) 307 [astro-ph/0603494] [INSPIRE].

[132] Y.Y.Y. Wong, *Neutrino mass in cosmology: status and prospects*, *Ann. Rev. Nucl. Part. Sci.* **61** (2011) 69 [arXiv:1111.1436] [INSPIRE].

[133] M. Archidiacono, T. Brinckmann, J. Lesgourgues and V. Poulin, *Physical effects involved in the measurements of neutrino masses with future cosmological data*, *JCAP* **02** (2017) 052 [arXiv:1610.09852] [ɪɴSPIRE].

[134] C. Cartis, J. Fiala, B. Marteau and L. Roberts, *Improving the flexibility and robustness of model-based derivative-free optimization solvers*, arXiv:1804.00154.

[135] C. Cartis, L. Roberts and O. Sheridan-Methven, *Escaping local minima with derivative-free methods: a numerical investigation*, arXiv:1812.11343.

[136] M.J.D. Powell, *The BOBYQA algorithm for bound constrained optimization without derivatives*, Technical Report 2009/NA06, DAMTP, University of Cambridge, U.K. (2009).

[137] J. Torrado and A. Lewis, *Cobaya: code for bayesian analysis of hierarchical physical models*, arXiv:2005.05290 [ɪɴSPIRE].

[138] F. Cooper and G. Venturi, *Cosmology and broken scale invariance*, *Phys. Rev. D* **24** (1981) 3338 [ɪɴSPIRE].

[139] C. Wetterich, *Cosmologies with variable newton's 'constant'*, *Nucl. Phys. B* **302** (1988) 645 [ɪɴSPIRE].

[140] F. Finelli, A. Tronconi and G. Venturi, *Dark energy, induced gravity and broken scale invariance*, *Phys. Lett. B* **659** (2008) 466 [arXiv:0710.2741] [ɪɴSPIRE].